ISET Journal of Earthquake Technology, Paper No. 583, Vol. 60, No. 4, December 2023, pp. 127-156

GROUND RESPONSE ANALYSIS AND ESTIMATION OF LIQUEFACTION POTENTIAL OF A SITE FOR NEAR FIELD AND FAR FIELD EARTHQUAKE MOTIONS

Ranjan Kumar (Corresponding author)
Engineering Services Group, Bhabha Atomic Research Centre
& Associate Professor, Homi Bhabha National Institute
E mail id: *ranjancv42@gmail.com*

Nikhil Gupta
Chemical Technology Group, Bhabha Atomic Research Centre, Mysore
E mail id: *ngupta@barc.gov.in*

Kapilesh Bhargava
Engineering Services Group, Bhabha Atomic Research Centre
& Professor, Homi Bhabha National Institute
E mail id: *kapil_66@barc.gov.in*

ABSTRACT

In the recent past, studies on the effects of near field and far field earthquakes on liquefaction potential of a site attracted the attention of researchers. Evaluation of liquefaction potential of a project site is presented. Input soil properties are estimated by conducting in-situ tests and laboratory tests on disturbed/undisturbed samples obtained from 38 boreholes spread over 7 zones across the site. Liquefaction potential is evaluated using empirical method. It is observed that out of 38 boreholes, 4 boreholes are found to be critical against liquefaction. The effects of near field and far field earthquake on liquefaction potential have been studied. Nine near field and seven far field free surface earthquake ground motions are converted into bedrock motions through deconvolution which is taken as input for detailed ground response analysis (GRA) of 4 critical boreholes. Soil behaviour is considered as equivalent linear and non-linear for GRA. Two boreholes are found to be liquefiable for some far field earthquakes and the other two are found to be safe for all earthquakes. The results have been compared. Cyclic stress ratio (CSR) obtained from empirical and GRA method is also compared and it is observed that values vary with regard to ground motions.

KEYWORDS: Liquefaction, Earthquake Ground Motion, Ground Response Analysis

INTRODUCTION

Evaluation of liquefaction resistance is an important aspect of Geotechnical Engineering. Soil sites are prone to liquefaction during earthquake. For establishment of various industrial facilities, potential site needs to be evaluated with regard to liquefaction. If the soil site is prone to liquefaction, engineering measures need to be taken to mitigate the same. During propagation of seismic waves, wave characteristics such as amplitude and frequency gets modified depending upon the soil properties. Structure needs to be designed properly for appropriate ground motion. Near field and far field earthquake ground motions affect the project site differently. Assumption of soil behaviour like linear, equivalent linear, non-linear during ground response analysis also affects the liquefaction potential result.

In the past, empirical and semi-empirical methods were developed which evolved over time. Empirical equation is used to predict stress generated due to earthquake loading and internal resistance of soil against this cyclic stress. Before 1981, total stress and shear stress criteria were used for assessment of liquefaction potential, after that shear stress ratio and resistant ratio were used for assessment of liquefaction potential. Cyclic Stress Ratio (CSR) is the stress generated due to earthquake loading, and Cyclic Resistance Ratio (CRR) is the resistance of soil against this earthquake loading. Factor of safety against liquefaction is the ratio of CRR and CSR. Dobry et al. (1981) defined factor of safety against liquefaction by the ratio of threshold acceleration for realization of liquefaction to maximum ground acceleration during the earthquake. Seed and Idriss (1981) defined factor of safety against liquefaction as the ratio of required periodic limit shear stress for starting of liquefaction at a specific soil and the average shear stress that a specific earthquake generates. Iwasaki et al. (1983) used liquefaction index criteria for assessment of liquefaction potential. The authors defined factor of safety against liquefaction as the ratio of periodic shear strength ratio to liquefy soil and shear stress ratio at higher magnitude earthquake. Tokimatsu and Yoshimi (1983) used cyclic stress ratio and cyclic resistance ratio for assessment of liquefaction potential. As per Youd and Idriss (2001), CSR is evaluated by empirical equation provided by them and CRR is evaluated by various field test data like Standard Penetration Test (SPT) value, Cone Penetration Test (CPT) value and shear wave velocity etc. Idriss and Boulanger (2006) presented the semi-empirical procedures for evaluating liquefaction potential during earthquakes. Sesov et al. (2012) performed laboratory experiments to find out liquefaction potential for a heterogeneous soil condition. Rakesh et al. (2016) evaluated liquefaction susceptibility of various site in Krishna district of Andhra Pradesh based on SPT and output of this study presented zig zag profile of factor of safety.

Ground response analysis is used to predict response of soil deposit to the motion of the bed rock which is immediately beneath it. Instead of using empirical method, detailed ground response analysis can be used for estimating the earthquake loading. In this technique, effect of soil stress-strain behaviour (i.e. Linear, equivalent linear, and non-linear), shear strength, particle size is also considered for estimation of earthquake loading. Kramer (2003) elaborated ground response analysis to predict response of soil deposit to the motion of the bed rock which is immediately beneath it. Bolisetti et al. (2014) compared different method like non-linear method, equivalent linear method and linear method of ground response analysis. Difficulty associated in various software used in ground response analysis was also described by authors. Hashash et al. (2017) developed DEEPSOIL V 7.0 which is a one-dimensional site response analysis program that generates acceleration, velocity, displacement time history as well as the response spectrum and Fourier amplitude spectrum for the selected motion or the imported motions. It has options of nonlinear time domain analyses with and without pore water pressure generation, equivalent linear frequency domain analyses including convolution and deconvolution, and linear time and frequency domain analyses. In the present study, this program is used for ground response analysis.

Effect of near field and far field earthquake ground motions have been studied in the past. Malhotra (1999) carried out study on response of building due to near field ground motion. Boominathan et al. (2000) determined factor of safety for far field ground motion and observed that factor of safety against liquefaction for sandy soil layers is much higher than 1.0 and for silty sandy layer, is marginally above 1.0. Paul (2005) evaluated the ground response parameters near the fault in rock considering the effects of faults and its orientation. Different observations have been made for near field and far field motions. Ambraseys and Douglas (2003) provided attenuation relationship of peak ground acceleration (PGA) by selecting 186 near field data. The attenuation relationship was developed after taking in to account the local site conditions. Further study was carried out by Mammo (2005), Sitaram (2007), Maheshwari et al. (2008), Davoodi et al. (2012), and Heydari and Mousavi (2005). Different observations have been made for near field and far field motions. This variation is caused by several factors e.g. site conditions, methodology of evaluation of ground response, distance and orientation of fault at site etc.

In the present paper, liquefaction potential is evaluated using empirical and analytical method for a coastal site. Far field and near field motions have been considered in analytical method. Equivalent linear and non-linear behaviour are considered in analytical method. The results have been summarized and compared.

SITE CHARACTERISTICS

This present soil site is near coastal area in south India which lies in seismic zone II as per Indian Standard IS 1893 (Part I)-2016. The type of soil in this site is marine deposits along the coast and aeolian deposits of red sand Teri and other types of sand near the coast. The formation of Teri is made up mainly of red stained quartz with an admixture of fine red clayey dust and fine grains of iron ore. There are various tests conducted on this site and liquefaction potential is evaluated by using Standard Penetration test (SPT) N value.

Drilling of 38 Bore Hole (BH) has been carried out up to 30 m depth. Layout of these boreholes is given in Figure 1.

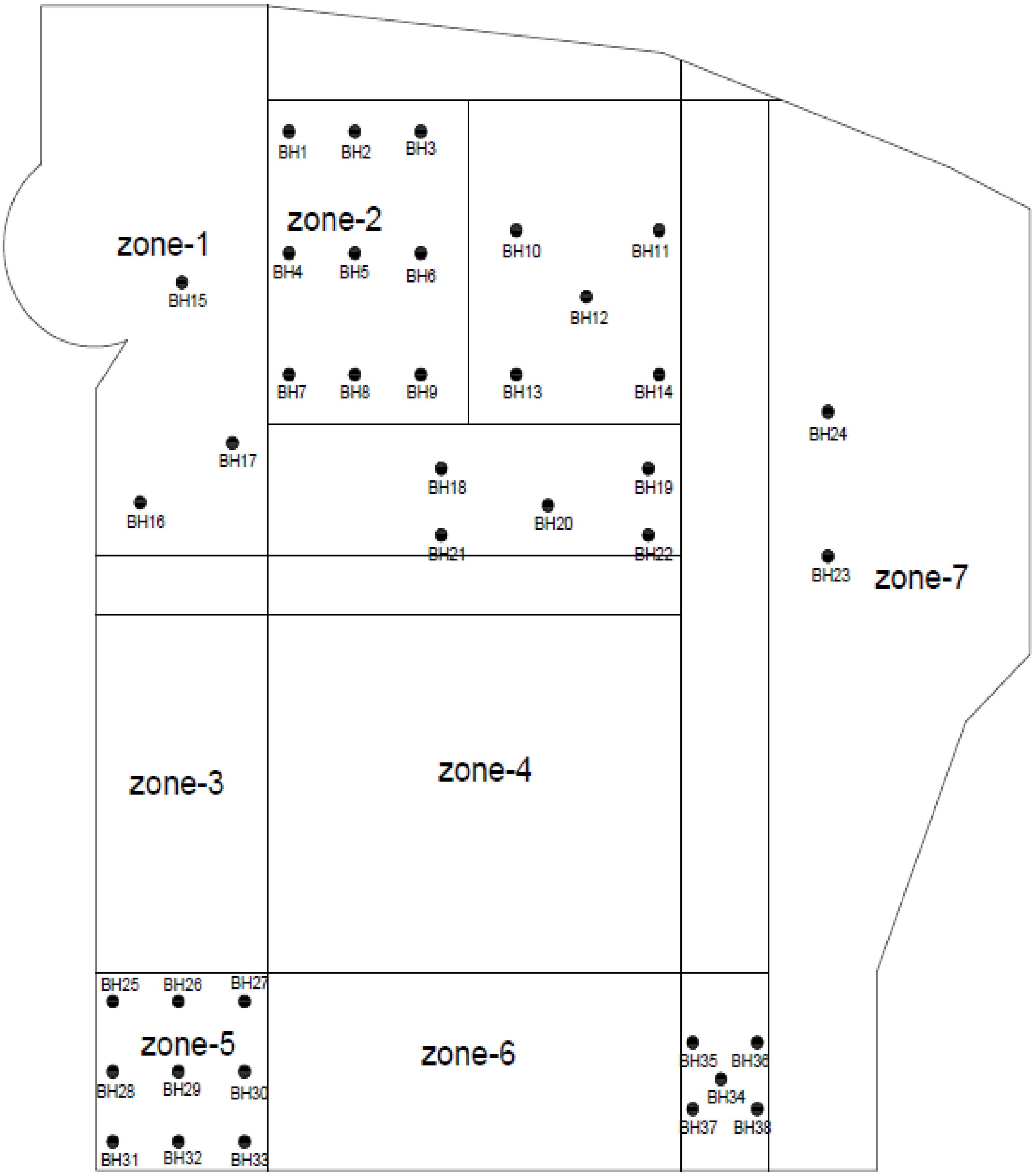

Fig. 1 Plan view of location of boreholes

SPT data are available for all these bore holes. The refusal of test has been considered when the penetration is not possible with 50 number of blows. Liquefaction potential for these 38 bore holes has been evaluated. Typical soil profile for a reference bore hole BH 14 is shown in Figure 2.

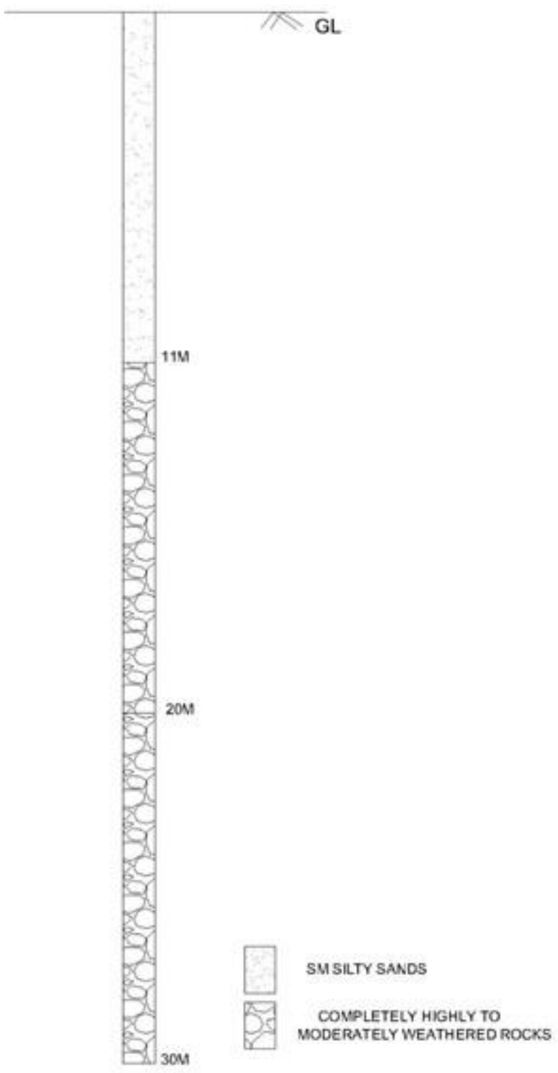

Fig. 2 Typical Soil profile of BH 14

LIQUEFACTION POTENTIAL BY EMPIRICAL METHOD

Liquefaction assessment by empirical method is carried out for all 38 boreholes. Procedure given by Youd and Idriss (2001) is adopted for liquefaction assessment. This paper is an update of Simplified empirical procedure for evaluating soil liquefaction. The author follows summary report of NCEER workshop on (1996) and NCEER/NSF workshop (1998) given by Youd et al. (1997). According to this, for evaluation of liquefaction resistance of soil, two variables are required:

- Seismic demand on a soil layer, express as CSR
- The capacity of soil to resist liquefaction, express as CRR

1. Evaluation of CSR by Empirical Method

CSR calculated by following empirical equation

$$\mathrm{CSR} = 0.65\left(\frac{a_{max}}{\mathrm{g}}\right)\left(\frac{\sigma_v}{\sigma_v'}\right)\mathrm{r_d} \tag{1}$$

Where,

z = depth below the ground surface

a_{max} = peak ground acceleration (PGA) in terms of g,

g = acceleration due to gravity

$\mathrm{r_d}$= stress reduction coefficient

$$\text{If, } z \le 9.15\, m,\ r_d = 1 - 0.00765z$$
$$\text{Else, } r_d = 1.174 - 0.0267z$$

σ_v and σ_v' are total and effective stress respectively.

If value of PGA is not available, the ratio a_{max}/g may be taken from seismic zone factor Z.

2. Evaluation of $CRR_{7.5}$

$CRR_{7.5}$ is the resistance provided by soil against stress generated due to 7.5 magnitude earthquake. However, laboratory test is available for evaluating CRR. But this test is applicable for undisturbed sample. It is uneconomical to obtain undisturbed sample. Hence, field tests are preferable for liquefaction assessment. Standard penetration test (SPT), Cone penetration test (CPT) and Shear wave velocity measurement (V_s) are common field tests for liquefaction assessment.

3. Calculation of CRR using the Value of SPT

Measured Blow Count, N_m of the SPT needs to be corrected for the standard conditions of equipment and overburden pressure. If the procedure is not standard, then various correction factors is multiplied to the measured blow count Nm

$$(N_1)_{60} = N_m C_N C_E C_B C_R C_S \tag{2}$$

Where, C_N, C_E, C_B, C_R and C_S are the corrections for overburden pressure, hammer energy, hammer efficiency, borehole diameter, rod length and non-standardised sampler respectively.

4. Influence of Fine Content on CRR

It is observed that CRR is increased with increase in fine content in soil. The authors developed an empirical equation to account the fine content. It is accounted by correcting $(N_1)_{60}$ to an equivalent clean sand value $(N_1)_{60cs}$ as follows.

$$(N_1)_{60cs} = \alpha + \beta (N_1)_{60} \tag{3}$$

Where

$$\alpha = 0;\ \beta = 1 \quad \text{for FC} \le 5\% \tag{4a}$$

$$(\alpha = e^{\left(1.76 - \frac{190}{(FC)^2}\right)} \beta = 0.99 + \frac{1.5\,(FC)}{1000} \qquad \text{For } 5\,\% < \text{FC} < 35\% \tag{4b}$$

$$\alpha = 5;\ \beta = 1.2 \text{ for FC} \ge 35\% \tag{4c}$$

After applying clean sand correction, following equation is used to estimate $CRR_{7.5}$ where $(N_1)_{60cs}$ shall be used instead of $(N_1)_{60}$.

$$CRR_{7.5} = \frac{1}{34 - (N_1)_{60cs}} + \frac{(N_1)_{60cs}}{135} + \frac{50}{[10(N_1)_{60cs} + 45]^2} - \frac{1}{200} \tag{5}$$

Where $(N_1)_{60cs}$ is corrected value of blow count after applying fineness correction and other corrections.

This equation is valid for $(N_1)_{60} < 30$

For $(N_1)_{60} \ge 30$, soil is classified as non-liquefiable.

5. Magnitude Scaling Factors (MSF)

For other than 7.5 magnitude earthquake, calculated value of CRR needs to apply correction. Calculated value of CRR at 7.5 magnitude earthquake is multiplied by a MSF. This MSF is calculated from following equation.

$$\text{MSF} = \frac{10^{2.24}}{M_w^{2.56}} \tag{6}$$

Where

M_w is the magnitude of earthquake.

$$CRR = CRR_{7.5} \times (\text{MSF}) \tag{7}$$

CSR is calculated considering water table at ground level. As per IS 1893 Part I (2016), for seismic zone II, the value of a_{max}/g is taken as 0.1. For $CRR_{7.5}$ calculation, SPT value should be in corrected form. Corrections C_N, CE, C_B, CR, CS and correction for fine content are applied on SPT blow count. As per National Disaster Management Authority (NDMA) report (2010), for this soil site, design earthquake magnitude is taken as 6.5. Summary of results obtained from empirical method with factor of safety (FOS) is given in Table 1.

Table 1: Summary of liquefaction assessment by empirical method

Bore Hole no.	Depth, m	CSR	CRR	FOS
1	1.00 - 1.45	0.189	Not liquefy	-
2	3.00 - 3.45	0.157	0.409	2.606
3	1.00 - 1.45	0.170	0.353	2.073
4	1.50 - 1.95	0.168	Not liquefy	-
5	1.50 - 1.95	0.163	0.309	1.893
6	3.00 - 3.45	0.164	Not liquefy	-
7	1.50 - 1.95	0.173	0.598	3.451
8	1.50 - 1.95	0.190	Not liquefy	-
9	1.5 - 1.95	0.175	Not liquefy	-
10	2.00 - 2.45	0.174	Not liquefy	-
11	2.00 - 2.45	0.157	Not liquefy	-
12	1.5 - 1.95	0.175	0.237	1.355
	4.5-4.95	0.171	0.646	3.778
13	1.5 - 1.95	0.183	0.369	2.014
14	**1.50 - 1.95**	**0.157**	**0.199**	**1.263**
	4.50 - 4.95	0.162	0.445	2.738
15	1.50 - 1.95	0.188	Not liquefy	-
16	1.50 - 1.95	0.159	0.224	1.411
	4.50 - 4.95	0.155	0.646	4.166
17	1.50 - 1.95	0.168	0.309	1.839
18	1.50 - 1.95	0.153	0.270	1.760
19	1.50 - 1.95	0.166	0.440	2.646
20	1.50 - 1.95	0.159	0.479	3.021
21	1.50 - 1.95	0.159	0.309	1.945
22	1.50 - 1.95	0.157	0.309	1.962
23	1.50 - 1.95	0.159	0.344	2.167
24	1.50 - 1.95	0.159	0.256	1.614
25	1.50 - 1.95	0.166	0.252	1.518
	4.50 - 4.95	0.171	0.321	1.879
26	**1.50 -1.95**	**0.173**	**0.212**	**1.226**
	4.50 - 4.95	0.175	0.306	1.750
27	1.50 - 1.95	0.166	0.353	2.123
28	1.50 - 1.95	0.181	0.252	1.394
	4.50 - 4.95	0.177	0.357	2.019
29	1.50 - 1.95	0.156	0.289	1.851
30	3.00 - 3.45	0.164	0.327	1.990
31	**1.50 - 1.95**	**0.173**	**0.212**	**1.226**
	4.50 - 4.95	**0.169**	**0.217**	**1.283**
	7.50 - 7.95	0.165	0.470	2.845
32	3.00 - 3.45	0.154	0.320	2.075
33	3.00 - 3.45	0.164	0.378	2.302

Bore Hole no.	Depth, m	CSR	CRR	FOS
	5.00 - 5.45	**0.162**	**0.184**	**1.138**
	9.00 - 9.45	0.159	0.246	1.544
	11.50 - 11.95	0.148	0.413	2.789
34	3.00 - 3.45	0.164	0.327	1.989
35	1.50 - 1.95	0.153	0.289	1.882
36	1.50 - 1.95	0.152	0.399	2.618
37	1.50 - 1.95	0.159	0.235	1.481
	4.50 - 4.95	0.155	0.279	1.801
38	1.50 - 1.95	0.166	0.288	1.730

It is observed from Table 1 that none of bore holes have FOS against liquefaction less than 1.0, if the site is subjected to an earthquake magnitude of 6.5. Hence, the site is not liquefiable. Also, as per IS 1893 part I (2016), for lesser earthquake related ground deformations (for important structures), FOS against liquefaction should be greater than 1.2. Hence, in the present study, FOS against liquefaction is considered as 1.2. It is observed from Table 1 that except for borehole no. 33, the FOS against liquefaction for other boreholes has been found to be more than 1.2, which is mainly attributed to higher SPT and bulk density values for the subsoil. For BH 33, the FOS against liquefaction is 1.138 at 5 – 5.45 m depth. It is also observed from Table 1 that FOS against liquefaction for bore hole nos. 14, 26 and 31 is 1.263, 1.226 and 1.226, respectively, at 1.5 – 1.95 m depth. Bore hole no. 33 is considered for detailed ground response analysis because FOS against liquefaction is found to be less than 1.2. Since FOS against liquefaction for bore holes 14, 26 and 31 is marginally (about 2 – 5 %) higher than 1.2, they are also considered for detailed ground response analysis.

Ground response analysis has been carried out for boreholes 14, 26, 31 and 33 considering the effects of far field and near field earthquake ground motion. The input data, e.g., SPT value, bulk density and % fine content for critical boreholes 14, 26, 31 and 33 are given in Table 2. It is mentioned that: (a) fines contents have been determined based on wet sieve analysis and hydrometer analysis of the soil samples taken at various depths of the bore hole, and (b) bulk density of soil has been determined based on laboratory test for undisturbed soil samples taken at various depths of bore hole.

Table: 2 Input data for critical Boreholes

BH no.	S. No.	Depth m	SPT value	Bulk density gm/cc	% Fines
14	1	1.50 - 1.95	13	1.69	7.37
	2	4.50-- 4.95	16	1.63	46.33
	3	6.00 - 6.45	23	1.63	37.7
	4	9.00 - 9.45	22	1.63	9.81
	5	10.50 - 10.95	36	1.63	9.81
	6	13.50 - 13.70	Refusal		
26	1	1.5-1.95	11	1.59	15.6
	2	4.5-4.95	15	1.56	15.6
	3	6-6.45	14	1.56	15.6
	4	9-9.45	14	1.56	15.6
	5	10.5-10.95	23	1.56	15.6
	6	13.5-13.95	22	1.56	35.14
	7	15-15.45	20	1.56	35.14
	8	18-18.25	Refusal		

31	1	1.50 - 1.95	11	1.59	15.6
	2	4.50 - 4.95	10	1.59	15.6
	3	7.50 - 7.95	21	1.59	15.6
	4	10.50 - 10.95	27	1.59	22.46
	5	12.00 - 12.45	14	1.69	22.46
	6	13.00 - 13.45	28	1.69	22.46
	7	14.00 - 14.45	35	1.69	22.46
	8	15.00 - 15.28	Refusal		
33	1	3.00 - 3.45	15	1.63	65.64
	2	5.00 - 5.45	10	1.63	9.15
	3	9.00 - 9.45	14	1.63	9.15
	4	11.50 - 11.95	26	1.69	9.15
	5	13.00 - 13.45	29	1.69	9.15
	6	14.50 - 14.95	30	1.69	9.15
	7	16.00 - 16.45	40	1.69	9.15
	8	18.00 - 18.15	Refusal		

FAR FIELD AND NEAR FIELD EARTHQUAKE GROUND MOTIONS

1. Definition

The difference between near field and far field earthquake can be referred from Uniform Building Code (UBC), 1997. If the epicentral distance of site is less than 15 km, it is near field (NF) earthquake and if it is more than 15 km than it is far field (FF) earthquake. Nine near field (NF-1 to NF-9) and seven far field (FF-1 to FF-7) earthquake ground motions are taken as input motions in this study from web source (www.strongmotioncentre.org). Location and epicentral distance from recording stations are given in Table 3 and Table 4.

Table 3: Location and epicentral distance of near field earthquake

S. No	Earthquake	Name or location of earthquake	Epicentral Distance
1	NF-1	Alum Rock California	10.9 Km
2	NF-2	Chi-Chi	10.7 Km
3	NF-3	Greece	13.7 Km
4	NF-4	Nishiakashi Japan	7.1 Km
5	NF-5	Takarazuka Japan	0.3 Km
6	NF-6	La-Habra Harborblvd at county line	5.1 Km
7	NF-7	Abbar, Iran	12.6 Km
8	NF-8	Elcentro, CA differential array	5.6 Km
9	NF-9	Chromioanapsiktirio Greece	12.1 Km

Table 4: Location and epicentral distance of far field earthquake

S. No.	Earthquake	Name or location of earthquake	Epicentral distance
1	FF-1	Bhuj, India	239 Km
2	FF-2	Chile	171 Km
3	FF-3	Gulf of California	95 Km
4	FF-4	Sumatra	392 Km
5	FF-5	Kaohsung, Taiwan	120 Km
6	FF-6	Fuk, Japan	158.6 Km
7	FF-7	Kardista, Greece	79.4 Km

2. Characteristics

Since input earthquake motion is measured from the past earthquake data, it may have non-zero displacement time history for the later part of motion. There is a need for base line correction which exhibits zero displacements time history. The site lies in seismic zone II and as per IS 1893, maximum surface acceleration at ground surface is taken as 0.1g. Hence, all earthquake motions are scaled to a PGA value of 0.1g.

3. Input Ground Motions

These input motions are measured at surface level. But for liquefaction and ground response study, it should be at bed rock level. Computation of bedrock motion from a known free surface motion is known as deconvolution. Transfer functions are used for deconvolution of free surface motions. Hence, deconvolution is needed in these input ground motions for computation of bedrock motion.

4. Calculation of Transfer Function

A uniform layer of isotropic, damped soil overlying rigid bed rock is considered. Harmonic horizontal motion of the bedrock will produce vertically propagating shear wave in the overlying soil.

The horizontal displacement can be expressed by using following equation of motion:

$$u(z,t) = Ae^{\iota(\omega t+k^* z)} + Be^{\iota(\omega t-k^* z)} \tag{8}$$

Where ω is the frequency of ground shaking, v_s^*

k* is the wave number (ω/v_s^*)

Where $v_s^* = (1+\iota\xi)v_s$

ξ is the Damping Ratio

At the free Surface (z=0), the shear stress and corresponding shear strain is zero

$$\tau\,(0,t) = G\gamma(0,t) = G\,\frac{\partial u(0,t)}{\partial z} = 0 \tag{9}$$

Substitute Equation (8) into Equation (9) and differentiate it out of this given the equation

$$u(z,t) = 2Acos(k^* z)\,e^{\iota\omega t} \tag{10}$$

It describes standing wave of amplitude 2Acoskz. Equation (10) can be used to define a transfer function that describes the ratio of displacement amplitudes at any two points in the soil layer. Choosing these two points to be top and bottom of the soil gives the transfer function.

$$|F_1(\omega)| = \frac{u_{\max\,(0,t)}}{u_{\max\,(H,t)}} = \frac{2Ae^{\iota\omega t}}{2Acos(k^* H)\,e^{\iota\omega t}} = \frac{1}{cos(k^* H)} = \frac{1}{\cos(\omega H/(1+\iota\xi)v_s)} \tag{11}$$

Input ground motion is applied at the ground surface and corresponding bed rock motion is computed. Since the present soil profile is a layered soil profile, series of ground motions are evaluated at the bottom of each soil layer to finally obtain the bedrock motion from the surface motion (Hashash et al 2017).

Soil Stress Strain behaviour is considered as Equivalent linear and non-linear. Equivalent linear analysis is linear analysis in which soil stiffness and damping characteristics are adjusted until they are compatible with the level of strain induced in the soil. In equivalent linear method, the actual nonlinear hysteretic stress-strain behaviour of cyclic loaded soil can be approximated by equivalent linear soil properties. The equivalent linear shear modulus, G is generally taken as secant shear modulus and the equivalent linear damping ratio ζ, as the damping ratio that produces the same energy losses in a single cycle as the hysteresis loop. Iteration towards strain compatible shear modulus and damping ratio in equivalent linear analysis (Kramer, 2003) is carried our as shown in Figure 3.

Using initial estimates of G_0 and ζ_0, the equivalent linear analysis predicts an effective shear strain γ_{eff1}. Because this strain is greater than those corresponding to G_0 and ζ_0, iteration is required. The next iteration use parameter G_1 and ζ_1 that are compatible with γ_{eff1}. The equivalent linear analysis is repeated and the parameters are checked until strain compatible value of G and ζ are obtained. In this study, fifteen no. of iterations are done to arrive at strain compatible values of G and ζ.

Non-linear analyses actually consider the non-linear inelastic stress-strain behaviour of soil by integrating the equation of motion in small time steps. At the beginning of each time steps, the stress strain relationship is referred to obtain the appropriate soil properties to be used in those time steps. By this method, a non-linear inelastic stress strain relationship can be followed in a set of small incrementally linear steps.

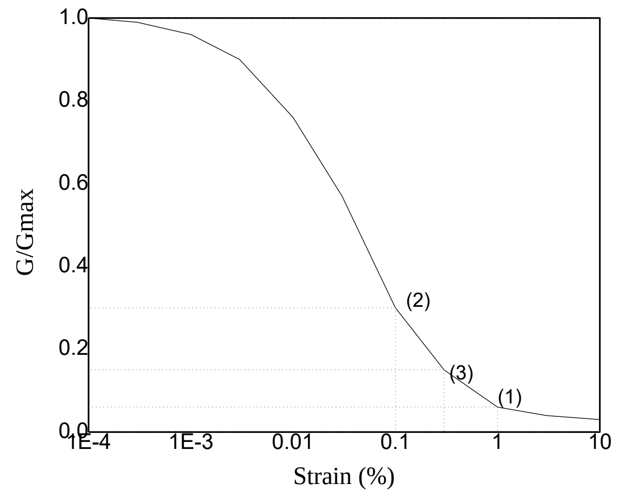

(a) Shear modulus

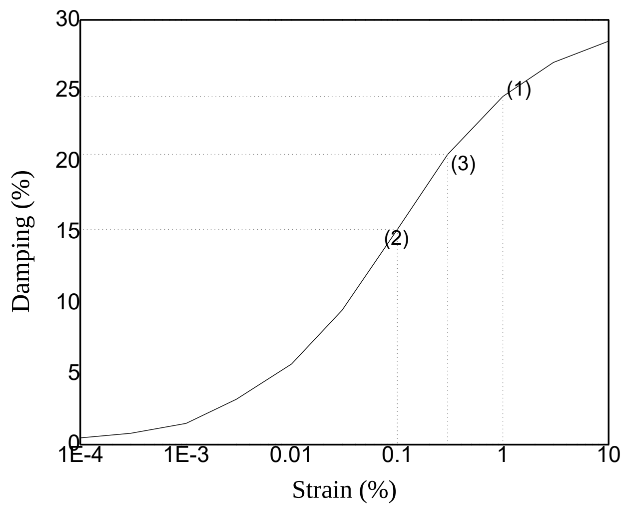

(b) Damping

Fig. 3 Iteration towards strain compatible shear modulus and damping ration in equivalent linear analysis (Kramer, 2003)

SITE SPECIFIC GROUND RESPONSE ANALYSIS (GRA)

For estimating CSR analytically, ground response analysis (GRA) needs to be done. There are various software tools like LS-DYNA (LSTC, 2009), SHAKE 2000 (Schnabel et al., 2012), DEEPSOIL 7.0 (Hashash et al., 2017) available for ground response analysis. In the present study, DEEPSOIL 7.0 (Hashash et al., 2017) software is used which can perform 1-D site specific ground response analysis using time domain non-linear analysis and frequency domain equivalent linear analysis by assuming excess pore water pressure. General quadratic hyperbolic (GQ/H) soil model is selected because it is suitable at large strain level. In this soil model. Stress strain relationship of soil is given by following equation.

$$\tau = \tau_{max}\left[\frac{1}{\theta_\tau}\left\{1+\left(\frac{\gamma}{\gamma_r}\right)-\sqrt{\left(1+\frac{\gamma}{\gamma_r}\right)^2-4\,\theta_\tau\left(\frac{\gamma}{\gamma_r}\right)}\right\}\right] \tag{12}$$

Where

τ = Shear Stress

γ = Shear Strain

τ_{max} = Shear strength of soil layer

$$\gamma_r(reference\ strain) = \frac{\tau_{max}}{G_o}$$

$$\theta_\tau = \theta_1 + \theta_2 \frac{\theta_4\left(\frac{\gamma}{\gamma_r}\right)\theta_5}{\theta_3{}^{\theta_5} + \theta_4\left(\frac{\gamma}{\gamma_r}\right)\theta_5} \tag{13}$$

θ_1 to θ_5 are the curve fitting parameters.

Further, modulus reduction and damping curve are fitted by mashing rules. Water Table is assumed at ground level to account for fluctuation in water level during earthquake. For estimation of value of shear modulus and damping ratio, the reference curve given by Seed and Idriss (1970) is considered which is suitable for sandy silty sand. Hence, it is taken as input reference curve.

Bedrock is assumed as rigid bedrock because earthquake motion was obtained from within the soil column. It implies a fixed end boundary at the base of soil layers. This rigid bedrock completely reflects any waves back through the soil layers.

LIQUEFACTION POTENTIAL USING GRA

As per soil investigation data for this site, bedrock is assumed at 13 m depth below GL. DEEPSOIL V 7.0 is used for analytical method. Under analytical method instead of SPT value, shear wave velocity data is required. These shear wave velocities are calculated from SPT values by empirical equation given by Anbazhaganet al. (2016). However, uncertainty analysis of this equation can be carried out by using methodology given by Zachariah and Jakka (2021) and Roy et al. (2018). Shear velocity from SPT N value is given by

$$V_s = 84.87N^{0.26} \tag{14}$$

CSR is calculated from Equation (1) where a_{max}/g is taken as 0.1 because this site lies in seismic zone II.

Calculation of shear wave velocity and CSR by empirical method is given in Table 5. For various depths, SPT N value is obtained and shear wave velocity corresponding to N value is estimated. Stress reduction coefficient r_d and CSR are estimated at corresponding depths.

The earthquake data taken in this study is measured at surface level and for one dimensional ground response analysis, acceleration time history is applied at bedrock level. Therefore, it is needed to convert this surface motion into bedrock motion. In frequency domain analysis deconvolution is used to convert input surface motion into bedrock motion by multiplying time history data to transfer function. The output of deconvolutions obtained for borehole 14 are shown in Figure 4 and Figure 5 and these are compared with original motions. It is observed that after deconvolution, maximum amplitude of earthquake at bedrock level is reduced.

Table 5: Calculation of shear wave velocity and CSR in BH 14

Sr. No.	Depth	N Value	Shear wave velocity by Anbazhagan et al. (2016) m/sec	Total stress (KN/m2)	Effective stress (KN/m^2)	r_d	CSR
1	1.5	13	165.341	24.86835	10.15335	0.9885	0.15738
2	4.5	16	174.512	72.83925	28.69425	0.9656	0.15932
3	6	23	191.780	96.8247	37.9647	0.9541	0.15817
4	9	22	189.576	144.7956	56.5056	0.9312	0.15509
5	10.5	36	215.473	168.78105	65.77605	0.8937	0.14905
6	13.5	Refusal		216.75195	84.31695	0.8136	0.13594

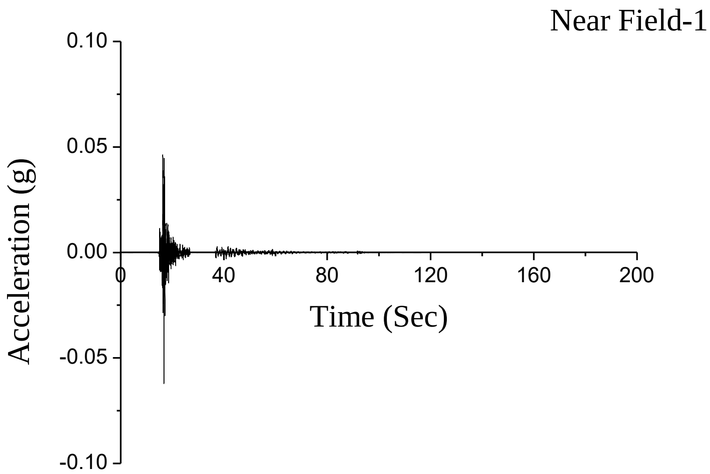
Near Field-1
Acceleration (g)
0.10
0.05
0.00
-0.05
-0.10
0
40
80
120
160
200
Time (Sec)

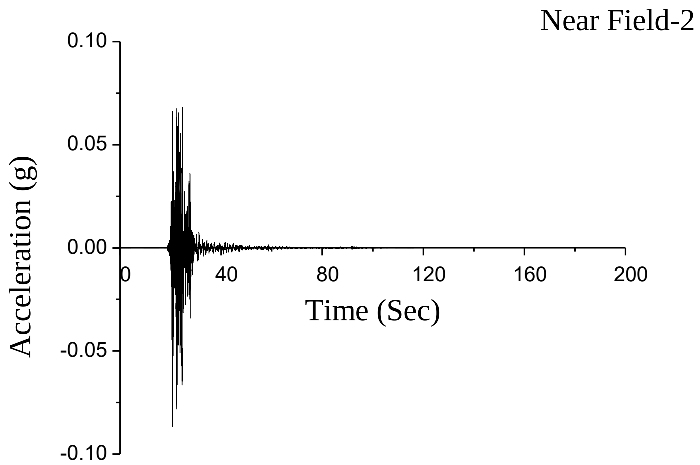
Near Field-2
Acceleration (g)
0.10
0.05
0.00
-0.05
-0.10
0
40
80
120
160
200
Time (Sec)

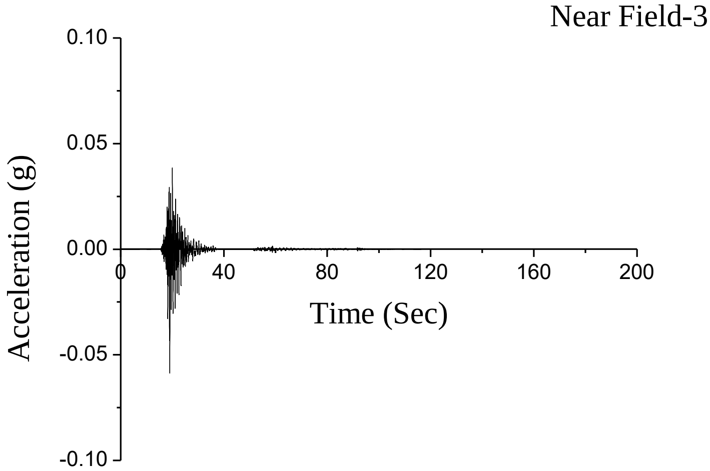
Near Field-3
Acceleration (g)
0.10
0.05
0.00
-0.05
-0.10
0
40
80
120
160
200
Time (Sec)

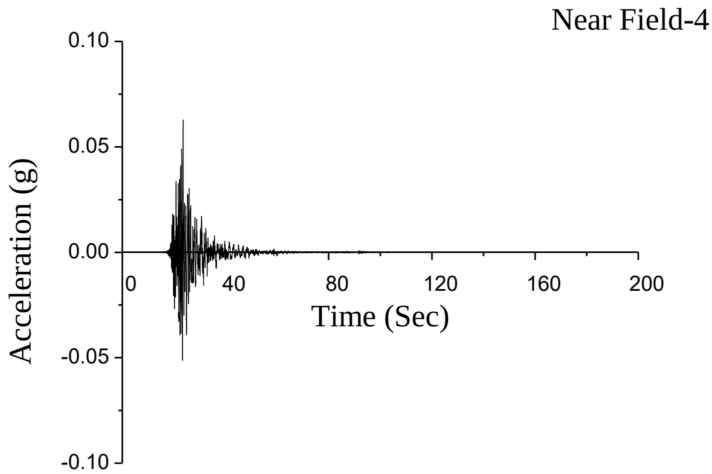
Near Field-4
0.10
0.05
0.00
-0.05
-0.10
Acceleration (g)
0
40
80
120
160
200
Time (Sec)

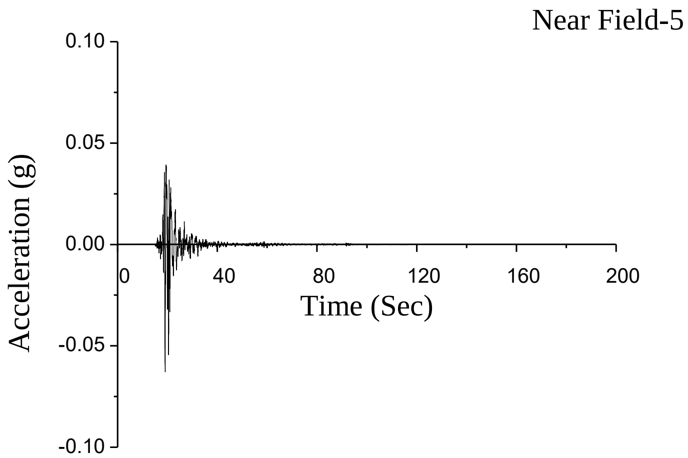
Near Field-5
0.10
0.05
0.00
-0.05
-0.10
Acceleration (g)
0
40
80
120
160
200
Time (Sec)

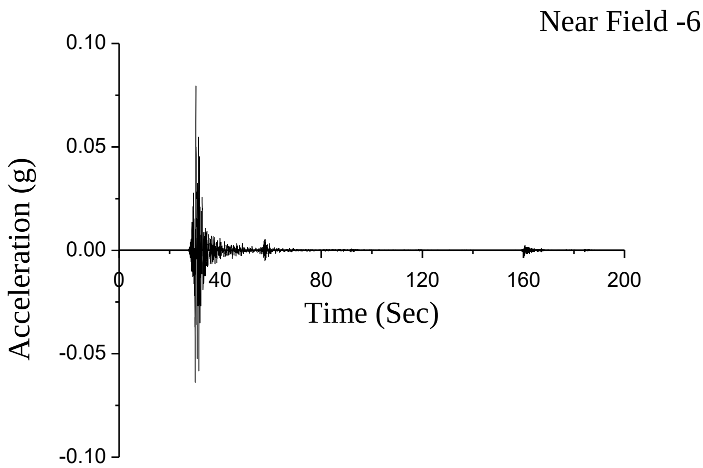
Near Field -6
0.10
0.05
0.00
-0.05
-0.10
Acceleration (g)
0
40
80
120
160
200
Time (Sec)

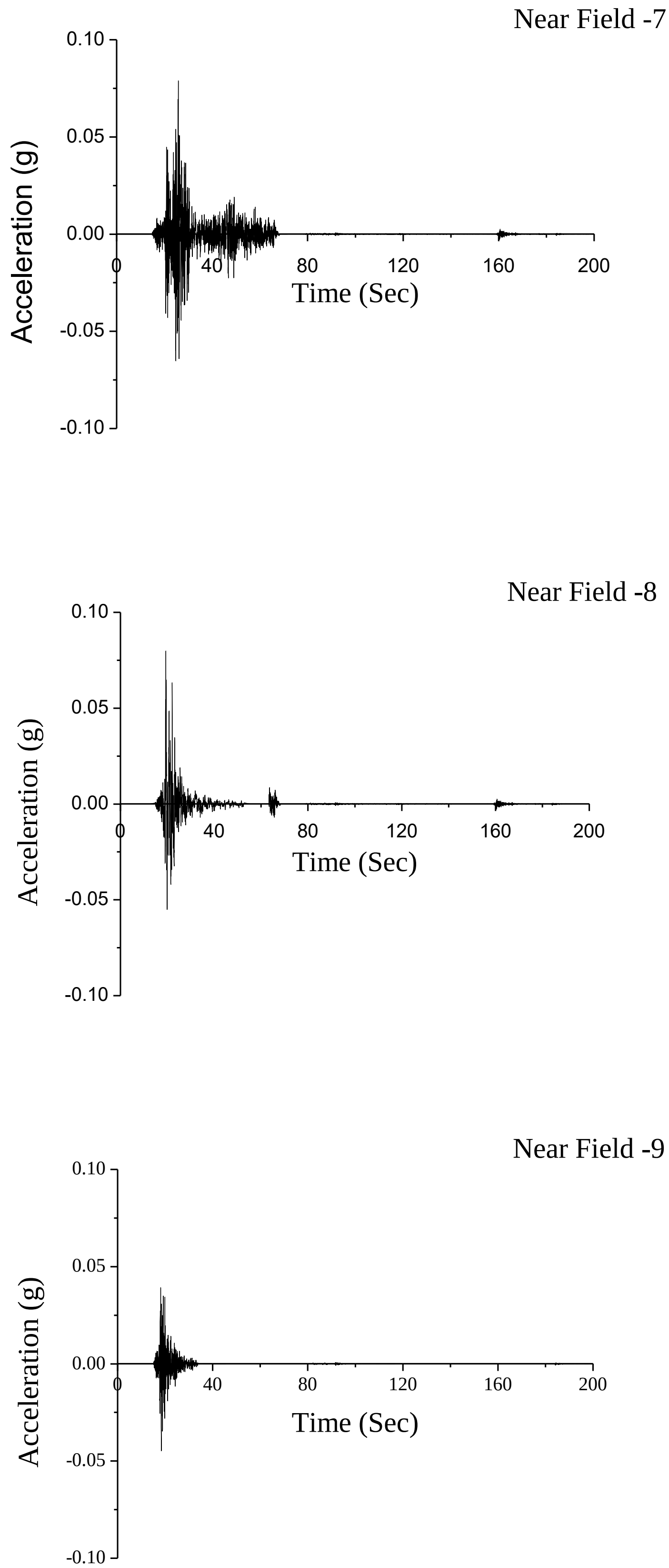

Fig. 4 Near field input bedrock motions for BH 14 after deconvolution of surface motion

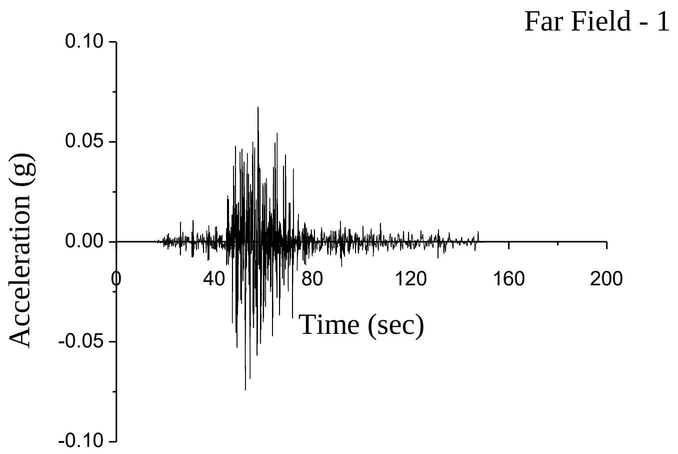
Far Field - 1
Acceleration (g)
Time (sec)

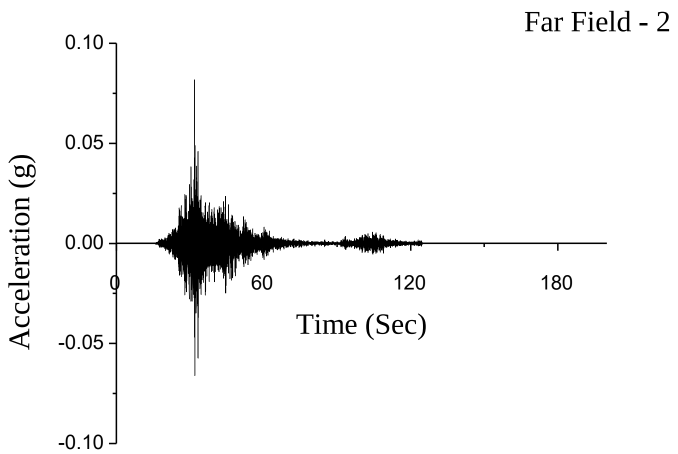
Far Field - 2
Acceleration (g)
Time (Sec)

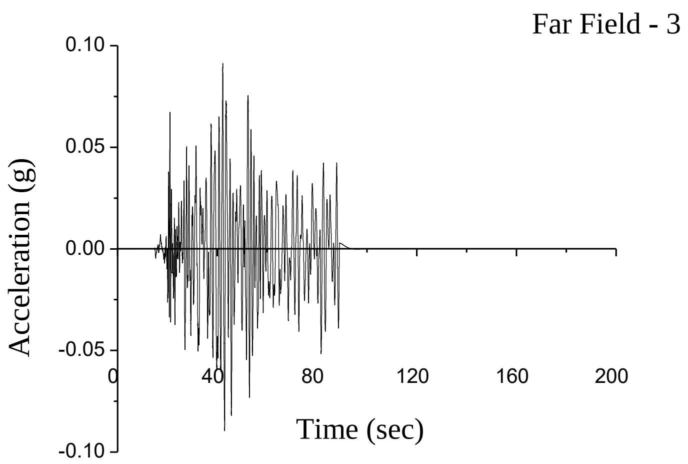
Far Field - 3
Acceleration (g)
Time (sec)

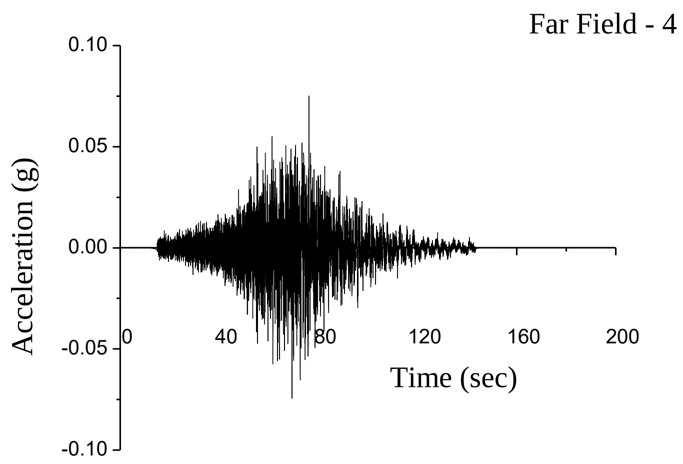
Far Field - 4
0.10
0.05
0.00
-0.05
-0.10
Acceleration (g)
0
40
80
120
160
200
Time (sec)

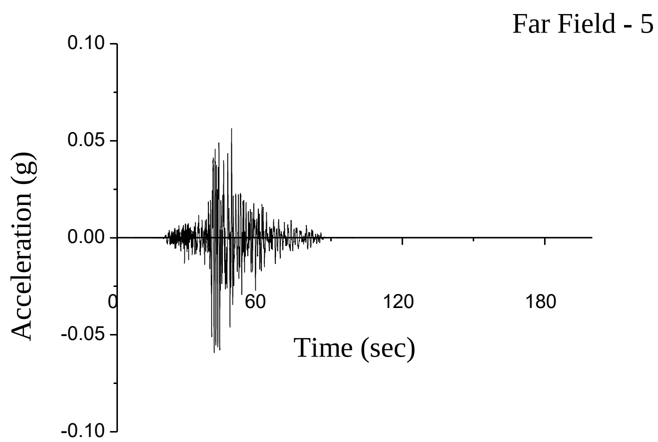
Far Field - 5
0.10
0.05
0.00
-0.05
-0.10
Acceleration (g)
0
60
120
180
Time (sec)

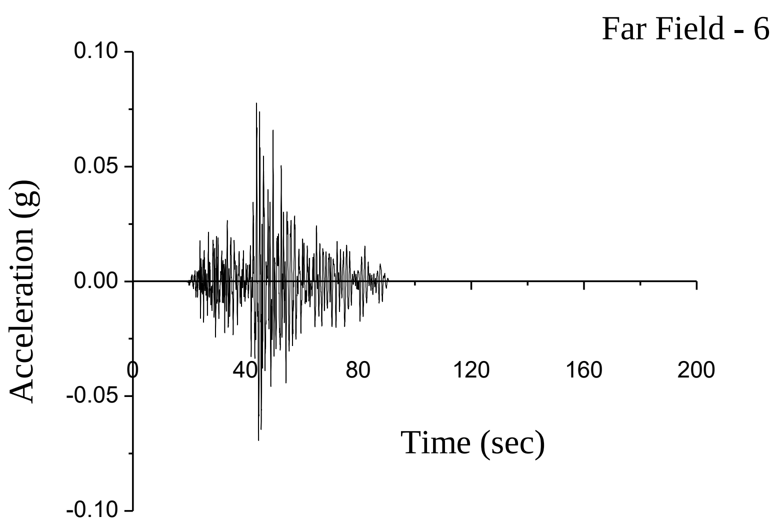
Far Field - 6
0.10
0.05
0.00
-0.05
-0.10
Acceleration (g)
0
40
80
120
160
200
Time (sec)

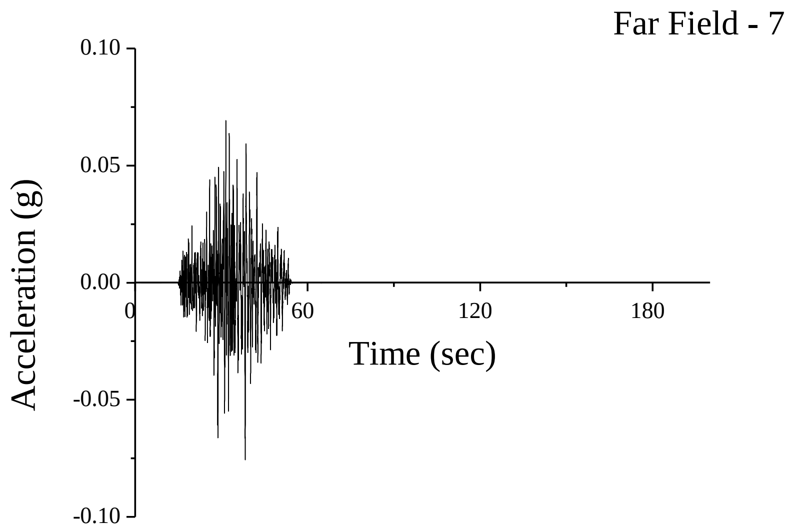

Fig. 5 Far field input bedrock motions for BH 14 after deconvolution of surface motion

Table 6: Dominant frequency, Arias intensity and significant duration

Earthquake	Dominant Frequency (Hz)	Arias Intensity	Significant Duration (Sec.)
FF-1	0.63	0.125	45-80
FF-2	13.48	0.04	18-75
FF-3	0.696	0.62	20-90
FF-4	18	0.34	15-132
FF-5	3.44	0.12	20-70
FF-6	0.65	0.55	20-90
FF-7	0.848	0.12	15-53
NF-1	7.5	0.05	20-30
NF-2	7	0.14	20-30
NF-3	4.75	0.75	16-26
NF-4	4.49	0.2	18-40
NF-5	0.6	0.38	17-30
NF-6	4.61	0.23	25-30
NF-7	4.46	0.2	15-60
NF-8	0.78	0.3	15-35
NF-9	4.38	0.055	15-30

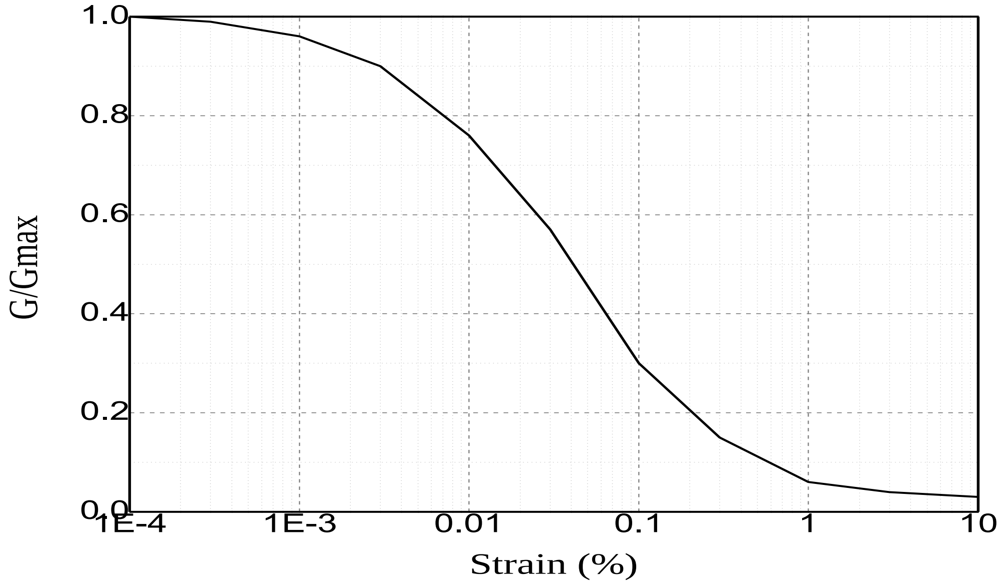

Fig. 6(a) G/G_{max} Vs Shear strain (%) curve at surface

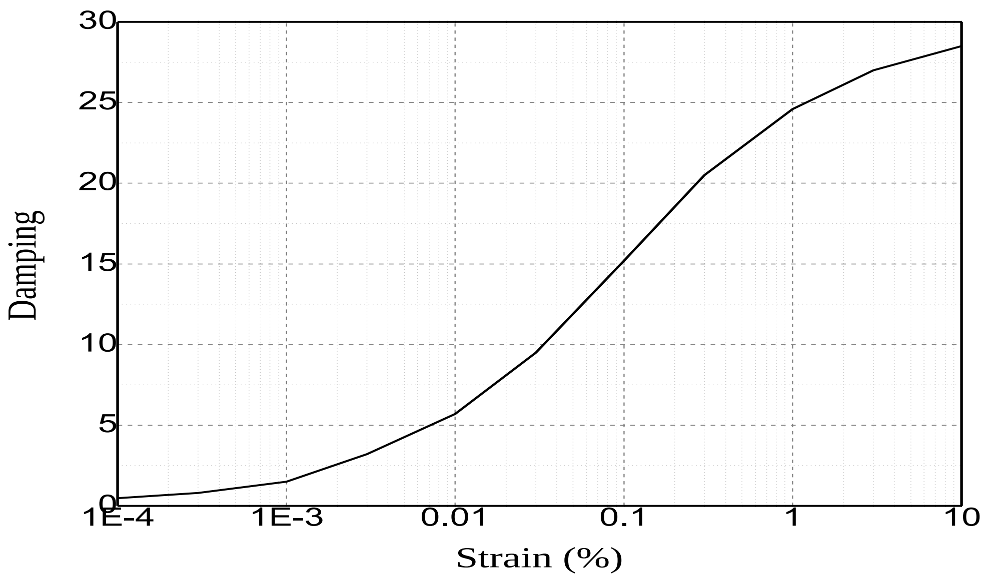

Fig. 6(b) Damping (%) Vs Shear strain (%) curve at surface

For all the near-field and far-field time histories considered in the study, PGA is scaled to 0.1g. Dominant frequency, Arias intensity and significant duration are presented in Table 6.

Further along with non-linear analysis, equivalent linear analysis is also performed using the option under complementary analyses. Under equivalent linear analysis, soil curve i.e. G/G_{max} Vs shear strain (%) curve and damping ratio Vs shear strain (%) curve at surface are taken as reference curve given by Seed and Idriss (1970), due to absence of cyclic triaxial test data for the soil site. Mean curves are given in Figure 6 (a) and Figure 6 (b). It is observed from these figures that shear modulus and damping of soil element vary with shear strain. At low strain, shear modulus is high but it decreases as strain increases and at low strain, damping is low but it increases as strain increases.

In nonlinear analysis, "General Quadratic / Hyperbolic Model (GQ/H)" soil model is considered. Dobry and Matasovic pore water pressure model of sand is used for pore pressure generation (Matasovic and Vucetic, 1993). The analyses have been carried out considering undrained condition. Shear stress Vs shear strain curve at 0.75 m and 2.25 m depth obtained from near field (NF-1) and far field (FF-1) earthquake are given in Figure 7 and Figure 8 respectively.

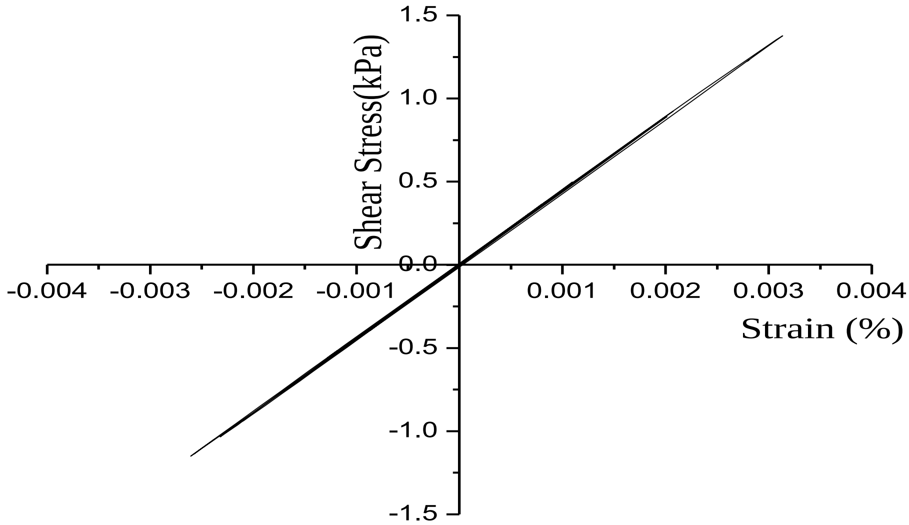

Fig. 7(a) Shear stress Vs Shear strain curve for BH 14 obtained from near field (NF-1) earthquake at 0.75 m from ground surface

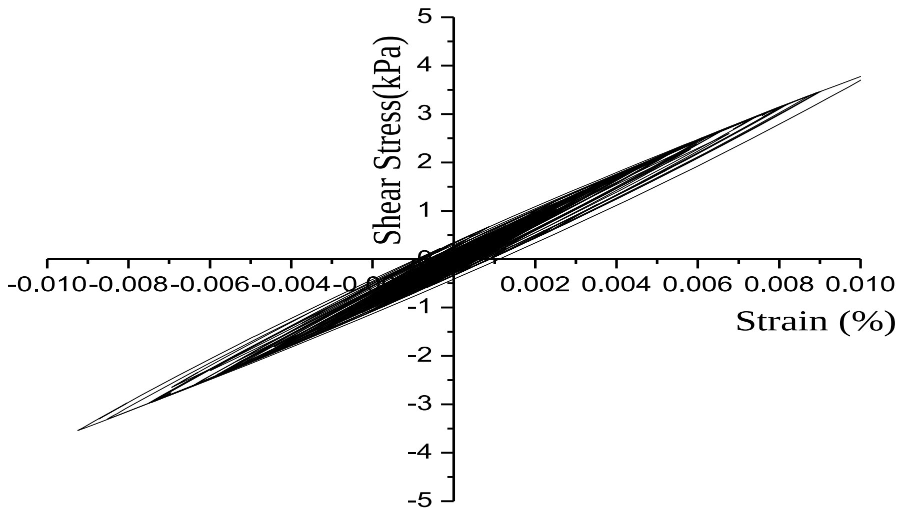

Fig. 7(b) Shear stress Vs Shear strain curve for BH 14 obtained from near field (NF-1) earthquake at 2.25 m from ground surface

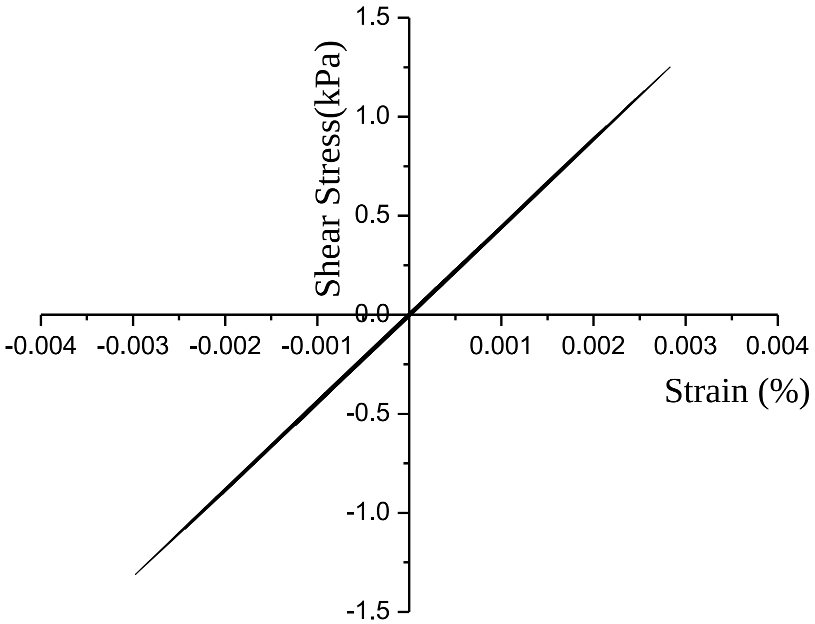

Fig. 8(a) Shear stress Vs Shear strain curve for BH 14 obtain from far field (FF-1) earthquake at 0.75 m from ground surface

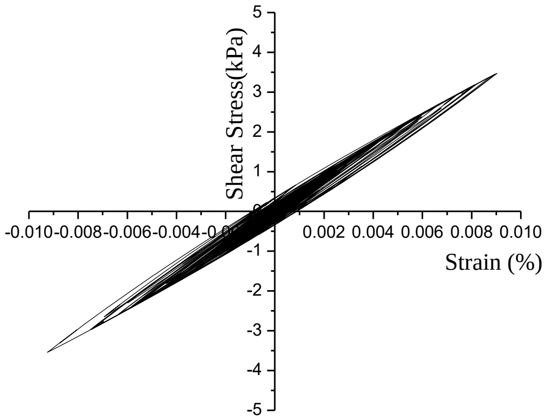

Fig. 8(b) Shear stress Vs Shear strain curve for BH 14 obtain from far field (FF-1) earthquake at 2.25 m from ground surface

It is observed in Figure 6 (a) that as shear strain increases, slope of the curve (G/G_{max} Vs Shear strain) decreases, i.e., shear modulus decreases. Figure 7 (a) is compared with Figure 7 (b), and Figure 8 (a) is compared with Figure 8 (b). It is seen that maximum strain and ratio of area of single loop of max strain to area of total strain energy in Figure 7 (b) and Figure 8 (b) are high as compared to those in Figure 7 (a) and Figure 8 (a). Damping (%) is proportional to ratio of area of single loop of max strain to area of total strain energy. Hence, damping (%) at max strain level in Figure 7 (b) and Figure 8 (b) is more than Figure 7 (a) and Figure 8 (a).

Analytical method estimates shear stress time history due to earthquake loading. This shear stress time history is divided by effective stress to convert the shear stress time history into shear stress/effective stress time history. This time history has number of peaks. CSR is the average value of these peaks which is taken as 0.65 times to maximum magnitude of peak. CSR values obtained from near field earthquakes, far field earthquakes and empirical method are compared. CSR by analytical method and empirical method are plotted as shown in Figure 9 and Figure 10. Nonlinear and equivalent linear analysis are considered in the analytical method.

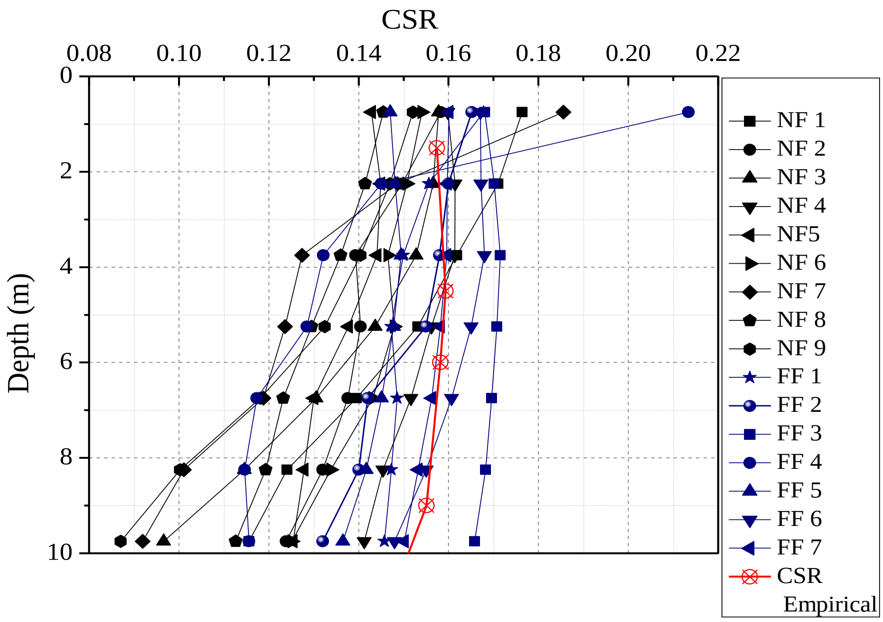

Fig. 9 Depth Vs CSR for BH 14 obtain by non-linear analysis

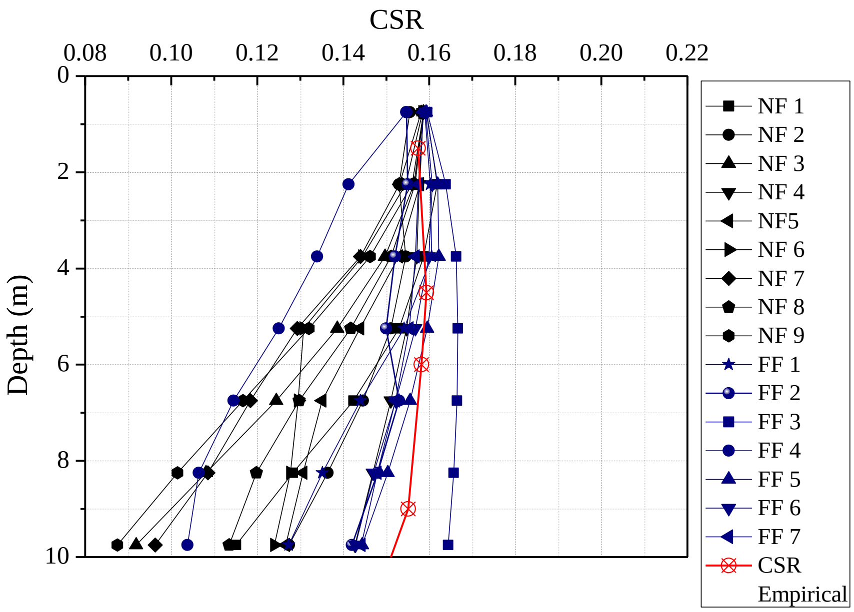

Fig. 10 Depth Vs CSR for BH 14 obtain by equivalent linear analysis

It is observed from Figure 9 and Figure 10 that variation in CSR value at surface level is more in non-linear analysis as compared to equivalent linear analysis. At greater depth, CSR obtained from analytical method is less than CSR obtained from empirical method. But at surface level, CSR obtained from far field and some near field earthquake is more than CSR obtained from empirical method. It means, with depth, stress is reduced to significant level if analysis is done by analytical method. It is observed that CSR obtained from far field earthquake is generally more than CSR obtained from near field earthquake in both non-linear and equivalent linear analysis except some cases. For each frequency content, far field earthquake has more data. Hence, sum of amplitude of acceleration is more. This may be the reason for more CSR values. NF-2 and NF-7 earthquake have higher CSR value as compared to some far field earthquakes. At this frequency, near field earthquakes have large acceleration level. It may be possible that value of transfer function is high.

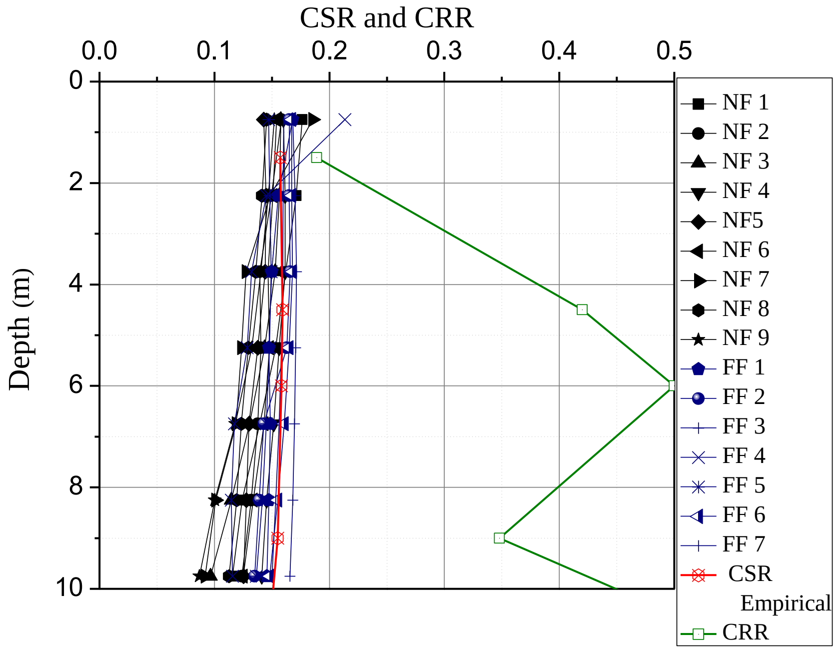

Fig. 11 CSR and CRR Vs depth for BH 14 obtained by non-linear analysis

Graph between CRR and CSR Vs depth is plotted in Figure 11 and Figure 12 for non-linear analysis and equivalent linear analysis respectively. Wherever CRR is less than CSR, that zone is susceptible to liquefaction.

For CRR calculation, SPT N value is considered in corrected form as per procedure given by Youd et al. (2001) and accordingly corrections for overburden pressure C_N, hammer energy efficiency C_E, borehole diameter C_B, rod length C_R, non-standardized sampler C_S and fine content are adopted. As shown in Figures 11 and 12, CRR is found to increase up to depth of about 6 m on account of increasing SPT values and presence of higher percent fines. Beyond depth of about 6 m CRR is found to decrease on account of substantial reduction in presence of percent fines.

It is observed in Figure 11 and Figure 12 that borehole 14 which is not liquefiable under empirical method, is liquefiable up to 1.5 m depth under non-linear analysis if FF-4 and NF-7 earthquake is subjected on this site. For remaining earthquakes, it is not observed liquefiable.

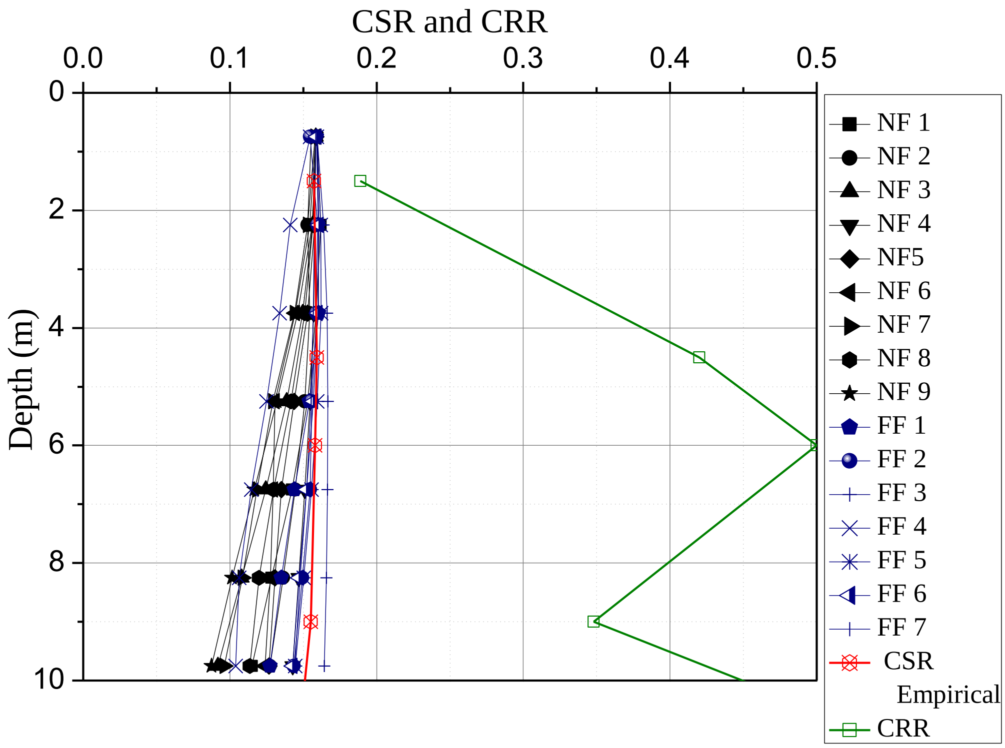

Fig. 12 CSR and CRR Vs depth for BH 14 obtained by equivalent linear analysis

1. Other results of BH14 by GRA

1.1 Depth Vs PGA

For non-linear analysis, output surface acceleration may amplify or de-amplify. It depends on characteristics of soil strata, frequency content and magnitude of acceleration at this frequency content. Figure 13 and Figure 14 are plotted for Depth Vs PGA for non-linear and equivalent linear analysis respectively.

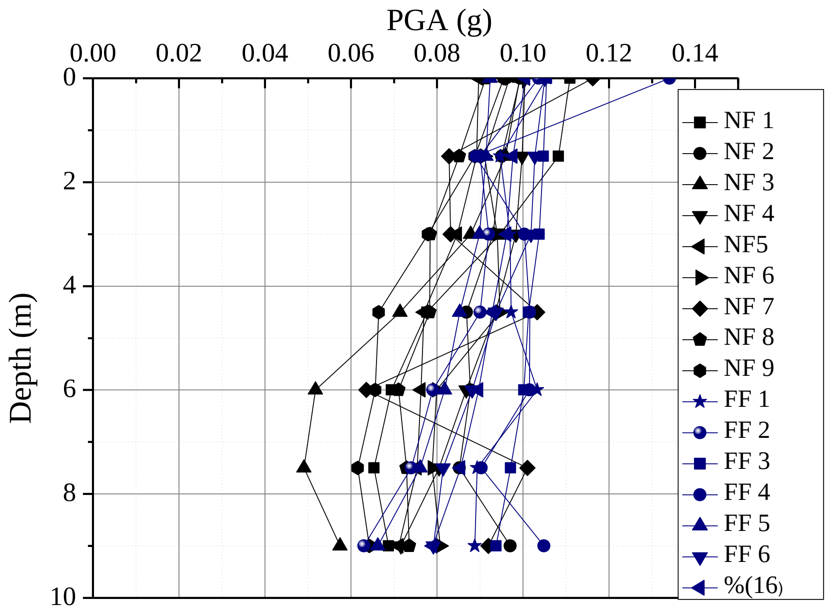

Fig. 13 Depth Vs PGA obtain from non-linear analysis for BH 14

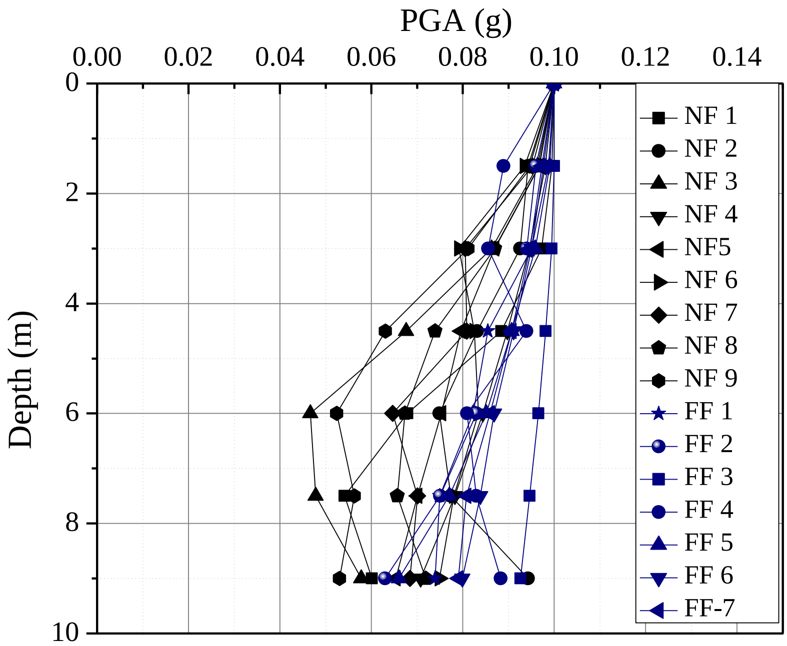

Fig. 14 Depth Vs PGA obtain from equivalent linear analysis for BH 14

For equivalent linear analysis, maximum surface acceleration is 0.1g for all near field and far field earthquakes, which is same as input motion surface acceleration; it may be due to deconvolution being carried out under equivalent linear analysis. It is also observed that PGA obtained from FF-4 earthquake is highest among other earthquakes in non-linear analysis. The PGA is observed to be minimum in trend at a depth of about 6 to 8 m for some of the far field and near field ground motions; this may be attributed mainly to shear wave velocity of the soil and the frequency of ground shaking at that depth.

1.2 Depth Vs Displacement

Depth Vs displacement plots are obtained from non-linear and equivalent linear analysis as shown in Figures 15 and 16 respectively.

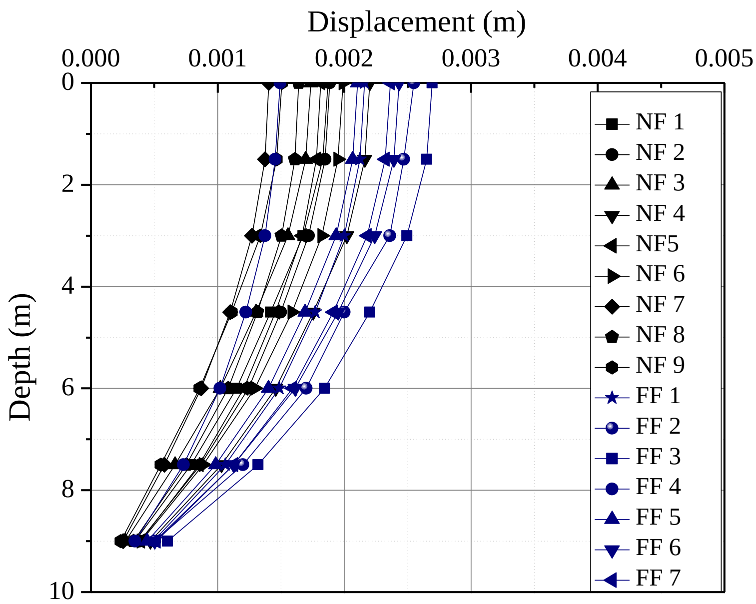

Fig. 15 Depth Vs displacement obtained from non-linear analysis

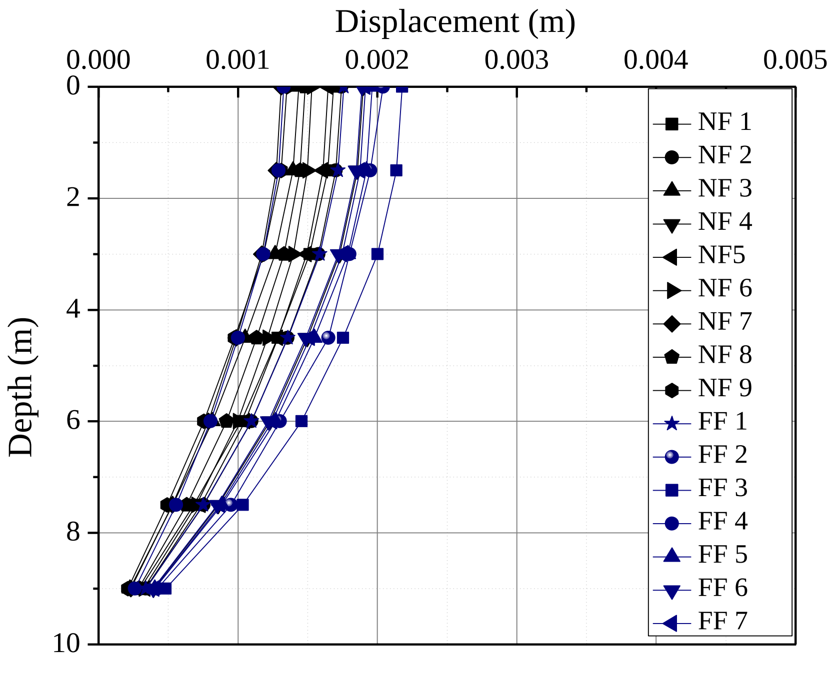

Fig. 16 Depth Vs displacement obtained from equivalent linear analysis

It is observed that maximum displacement is more in nonlinear analysis as compared to equivalent linear analysis. It also seen that for non-linear analysis and equivalent linear analysis, displacement is maximum at surface level and then it is reduced with depth. It is also observed that maximum displacement obtained for far field earthquakes is more than near field earthquakes.

1.3 Depth Vs Max. Strain

Depth Vs max strain plots are obtained from non-linear and equivalent linear analysis as shown in Figure 17 and 18 respectively.

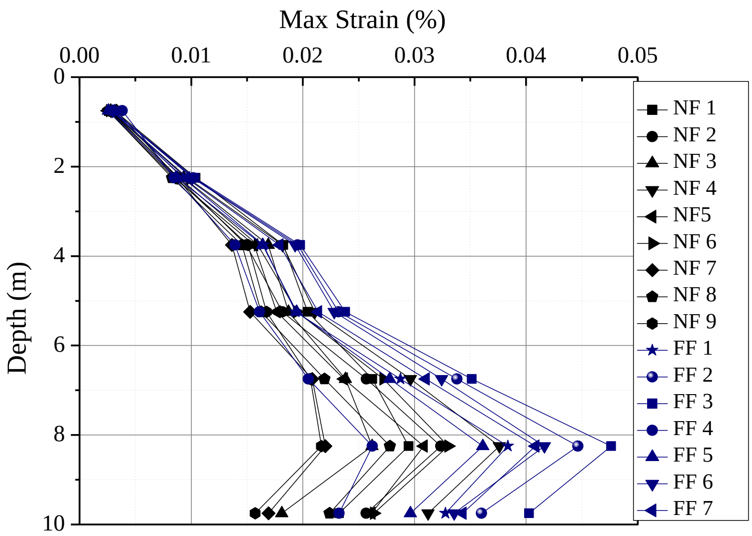

Fig. 17 Depth Vs maximum strain obtained from non-linear analysis

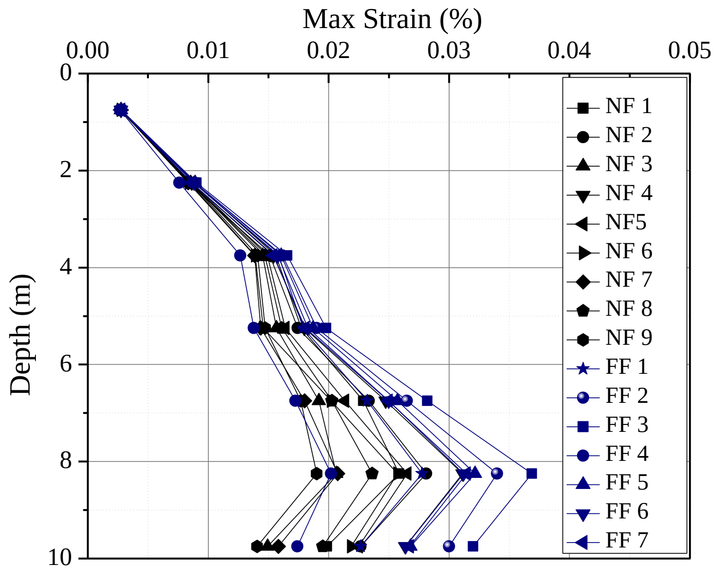

Fig. 18 Depth Vs maximum strain obtained from equivalent linear analysis

It is observed that max. strain is increased with increase in depth for both equivalent linear and non-linear analysis. It is also observed that strain obtained from non-linear analysis is more as compared to strain obtained from equivalent linear analysis. It is also observed that max. strain obtained from far field earthquakes is more than strain obtained from near field earthquakes and max strain obtained from FF-3 earthquake is highest among other earthquakes in both non-linear and equivalent linear analysis. The observed trend of shear strain may be attributed mainly to material properties of the soil, shear wave velocity of the soil and the frequency of ground shaking at that depth.

1.4 Peak Spectral Acceleration (PSA) Vs Period

PSA is the max. response of a single degree of freedom system subjected to a particular input motion. It is function of natural frequency and damping ratio of SDOF system. To carry out study on effect of earthquake characteristics on single degree of freedom system, PSA Vs period graphs are drawn for two near field earthquakes, NF-7 and NF-5, and two far field earthquakes, FF-4 and FF-5. The above earthquakes give maximum and minimum value of CSR under non-linear analysis for near field and far field earthquake respectively.

Figure 19 and Figure 20 graphs are plotted between peak spectral acceleration and period.

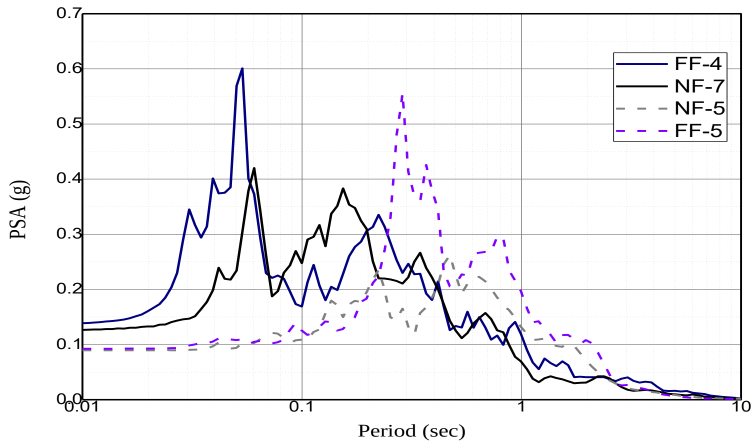

Fig. 19 Peak spectral acceleration Vs Period under non-linear analysis

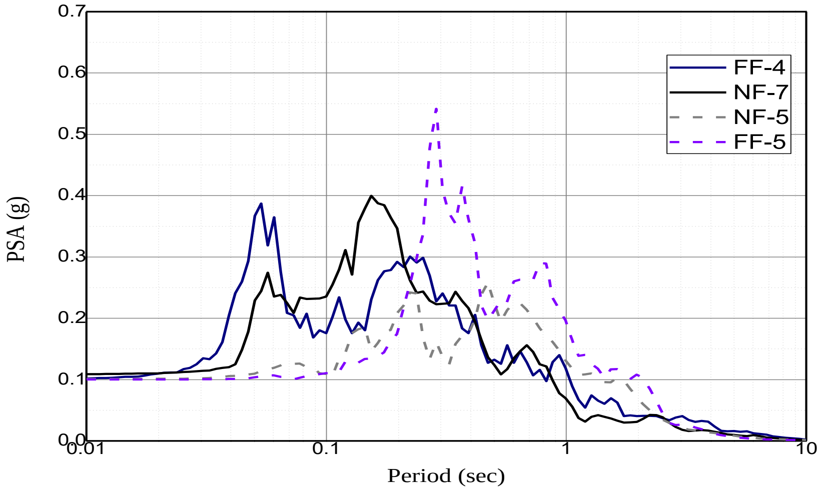

Fig. 20 Peak spectral acceleration Vs Period under equivalent linear analysis

PSA obtained from far field earthquake is greater than PSA obtained from near field earthquake under both non-linear and equivalent linear analysis. It may be due to far field earthquake having more frequency content than near field earthquake. Hence, response obtained from far field earthquake is more than near field earthquake.

1.5 Fourier Amplitude (g-sec) Vs Frequency

Plot of Fourier amplitude Vs frequency is known as Fourier amplitude spectrum. This Fourier amplitude spectrum shows that how amplitude of ground motion is described with respect to frequency. A point in Fourier amplitude represents sum of all amplitude at a particular frequency. Fourier amplitude spectrum has either narrow or broad spectra. Narrow spectra implies that motion has dominant frequency which can produce sinusoidal time history. Broad spectra implies irregular time history. Fourier amplitude graph at surface level for two near field, NF-5 and NF-7 and two far field, FF-4 and FF-5 in non-linear analysis are plotted. The above earthquakes give maximum and minimum value of CSR under non-linear analysis for near field and far field earthquake respectively.

It is observed that maximum Fourier amplitude obtained from far field earthquake is more than that obtained in near field earthquake. It may be due to far field having more data than near field for a particular frequency. Hence, sum of these data at a particular frequency is more in case of far field than near field earthquake.

2. Analysis of BH26

It is noted that earthquake data taken in this study is measured at surface level and for one dimensional ground response analysis, acceleration time history is applied at bedrock level. To convert this surface motion into bedrock motion, deconvolution is used in frequency domain analysis. After deconvolution, bedrock motion is applied as input earthquake motion for borehole 26, 31 and 33 in one dimensional analysis.

It is observed that CSR at top level obtained from FF-4 earthquake is highest among others but CSR obtained from FF-4 earthquake reduces significantly with depth. At greater depth CSR obtained from FF-3 earthquake is highest among others. Similar to BH 14, FF-2 earthquake shows unique variation with depth. It is also observed that CSR obtained from far field earthquakes is generally more than CSR obtained from near field earthquake. It may be due to far field earthquake having more frequency content as compare to near field earthquake. Hence, chances of amplification are more in case of far field earthquakes. Sometimes at dominating frequency of near field earthquake, peak value or sufficient magnitude of ground response may occur. Hence, NF-2 and NF-7 earthquake is amplifying more as compare to some far field earthquakes. If we compare result obtained from empirical method and analytical method, it is observed that at top level CSR obtained from far field earthquake is more than CSR obtained from empirical method and at greater depth CSR obtained from empirical method is more than CSR obtained from near field earthquake.

There is similar observation as in Figure 12. At top level, CSR obtained from equivalent linear analysis is almost same in analytical method and empirical method. It may be deconvolution being carried out under equivalent linear analysis only and input surface PGA is taken as 0.1g. At greater depth CSR obtained from far field earthquake is more than CSR obtained from near field earthquake. There is similar observation as in Figure 11 and Figure 12. CSR obtained from equivalent linear analysis is lesser than CSR obtained from non-linear analysis.

It is observed that under non-linear analysis, this borehole is liquefiable up to 1 m depth if FF-4 earthquake is subjected on it. Under equivalent linear analysis, borehole 26 is not observed liquefiable.

3. Analysis of BH31

It is observed that that CSR value at surface level for BH31 is more in nonlinear analysis as compare to equivalent linear analysis. It can be seen that CSR obtained from far field earthquake is generally more than CSR obtained from near field earthquake. It may be due to far field earthquake having more frequency content as compare to near field earthquake. Hence, chances of amplification are more in case of far field earthquakes. If we compare result obtained from analytical and empirical method, it can be seen that at top level, CSR obtained from non-linear analysis of far field earthquake is more than CSR obtained from empirical method. In equivalent linear analysis, CSR at top level obtained from empirical and analytical method is almost same. It may be deconvolution being carried out under equivalent linear analysis only. BH31 is not liquefiable as per the graphs obtained.

4. Analysis of BH33

CSR and CRR have been calculated similar to BH 14. Input data of this borehole is given in Table 2. At 19 m depth, refusal is observed in SPT. Hence, bedrock is assumed at 19 m depth. It is noted that observed N value after 16 m depth is more than 30. There is no chances of liquefaction as per Youd et al. (2001). Hence, in present case, liquefaction potential is calculated up to 16 m depth only. Calculation of shear wave velocity and CSR by empirical method is similar to as given in Table 5.

Variation in CSR value at surface level is more in non-linear analysis as compared to equivalent linear analysis. At surface level, in equivalent linear analysis, almost same value of CSR has been obtained. It may be due to deconvolution being carried out in equivalent linear method only. At greater depths, CSR obtained from analytical method is less (except for FF-3) than CSR obtained from empirical method but at surface level CSR obtained from far field and some near field earthquake is more than CSR obtained from empirical method. It means, with depth, stress is reduced to significant level if analysis is done by analytical method. It is observed that like other boreholes, CSR of FF-2 earthquake follows unique relation with depth than other earthquakes in both non-linear and equivalent linear analysis. It is also observed that CSR obtained from far field earthquake is generally more than CSR obtained from near field earthquake in both non-linear and equivalent linear analysis except some cases. It may be due to far field earthquake having more frequency content as compared to near field earthquake. Hence, chances of amplification are more in case of far field earthquakes. It is also observed that at top level, CSR observed from analytical method is more than CSR observed from empirical method.

It is observed that unlike other boreholes, this bore hole has more factor of safety against liquefaction at surface. But at depth 5 m, less factor of safety has been observed although this borehole is not observed liquefiable.

CONCLUSIONS

Evaluation of liquefaction potential of a project site is presented by empirical and analytical (GRA) methods and results are compared. Input soil properties are estimated by conducting in-situ tests and laboratory tests on disturbed/undisturbed samples obtained from 38 boreholes spread across the site. Out of 38 boreholes, 4 boreholes are found to be critical against liquefaction as per empirical method. The effects of nine near field and seven far field earthquake motions on liquefaction potential have been studied for 4 critical boreholes. All earthquake motions are scaled to 0.1g as per site zoning requirement. Soil behaviour is considered as equivalent linear and non-linear for GRA. Based on the present study, following conclusions are drawn:

1. For GRA, input ground motions at surface level are transferred to bed rock level through deconvolution. After deconvolution, reduction in amplitude is observed to be 20-40% for near field motions and 10-40% for far field motions. Soil layers have reasonable influence in modifying the ground response either in amplification or de-amplification. Surface amplification has been observed for six far field and two near field earthquake ground motions in case of non-linear analysis of soil. In case of equivalent linear analysis of soil, same surface PGA value i.e. 0.1g has been obtained for all the far field and near field earthquake ground motions, thus, resulting in no surface amplification.
2. CSR obtained from analytical (GRA) and empirical methods has been compared. Reduction of CSR with depth is more in analytical method as compared to empirical method. It may be due to consideration of soil stratification in case of analytical method. Therefore, increase in FOS against liquefaction has been observed in case of analytical method. CSR obtained from far field earthquake is generally more than that obtained from near field earthquake. For each frequency content, far field earthquake has more data. Hence, sum of amplitude of acceleration is more. This may be the reason for more CSR values. CSR is generally more in case of non-linear analysis which implies less value of FOS against liquefaction and confirms the necessity of this study. Variation of CSR at surface level is more in case of non-linear analysis of soil. In case of equivalent linear analysis of soil, FOS against liquefaction is found to be more than one for all 4 bore holes. BH14 is found to be liquefiable under non-linear analysis of soil for one near field and one far field motions at shallow depth. BH26 is found to be liquefiable under non-linear analysis of soil for one far field motion at shallow depth. As per GRA, other two boreholes are not liquefiable. Hence, selection of a particular earthquake for analysis is very important. Even if analysis is done with many earthquakes, results need to be compared with empirical method.
3. Detailed study of other parameters for all the four critical bore holes is also carried out. De-amplification of PGA with depth is found to be more in case of near field motion. For non-linear analysis of soil, both amplification and de-amplification has been observed at surface level and across the depth of soil strata for various near field and far field motions. In case of equivalent linear analysis of soil, there is de-amplification in all cases. Displacement across the depth of soil is found to be less in case of near field motion, and more in case of non-linear analysis of soil. It may be due to sum of amplitude of accelerations having more values in far field earthquakes for each frequency content. Displacement is found to be maximum at surface level and it reduces across the depth of soil strata. Maximum strain is found to be more across the depth and for non-linear analysis of soil, and less for near field motions. Peak spectral acceleration (PSA) is found to be more in case of non-linear analysis of soil and far field motions. Fourier amplitude is found to be more in case far field motions.

REFERENCES

1. Ambraseys, N.N. and Douglas, J. (2003). "Near-Field Horizontal and Vertical Ground Motion" *Soil Dynamics and Earthquake Engineering*, Vol. 23, No. 1, pp. 1-18.
2. Anbazhagan, P., Bajaj, Ketan, Reddy, G.R., Phanikanth, V.S. and Yadav, D.N. (2016). "Quantitative Assessment of Shear Wave Velocity Correlations in the Shallow Bedrock Sites" *Indian Geotech J*, Vol. 46, No. 4, pp. 381-397.
3. Bolisetti, Chandranath, Whittaker Andrew, S., Mason, H. Benjamin, Almufti, Ibrahim and Willford, Michael (2014). "Equivalent Linear and non-linear site response analysis for design and risk assessment of safety- related nuclear structure*" Nuclear Engineering and Design,275, 107–121.*
4. Boominathan, A., Koteswara Rao, P.C., Sivathanu Pillai, C. and Hari, S. (2000). "Measurement of Dynamic Properties and Evaluation of Liquefaction Potential of a 500mw Prototype Fast Breeder Reactor Site Located in South of India" *12 WCEE,* pp. 964.
5. Davoodi, M., Sadjadi, M., Goljahani, P. and Kamalian, M. (2012). "Effects of Near-Field and Far-Field Earthquakes on Seismic Response of SDOF System Considering Soil Structure Interaction" *WCEE 2012*DEEPSOIL V 7.0.
6. Dobry, R., Stokoe, K.H., Ladd, R.S. and Youd, T.L. (1981). "Liquefaction Susceptibility from S-Wave Velocity", *ASCE National Convention*, St. Louis, Missoiuri, USA, Preprint, pp. 81-544
7. Hashash, Y.M.A., Musgrove, M.I., Harmon, J.A., Ilhan, O.,Groholski, D.R., Phillips, C.A. and Park, D. (2017). "DEEPSOIL7.0, User Manual".

8. Heydari, M. and Mousavi, M. (2015). "The Comparison of Seismic Effects of Near-field and Far-field Earthquakes on Relative Displacement of Seven-storey Concrete Building with Shear Wall" *Current World Environment*, Vol. 10, Special Issue No. 1, pp. 40-46.
9. Idriss, I.M. and Boulanger, R.W. (2006). "Semi-Empirical Procedures for Evaluating Liquefaction Potential During Earthquakes" *Soil Dynamics and Earthquake Engineering*, pp. 115–130.
10. IS 1893 Part 1(2016). "Criteria for Earthquake Resistant Design of Structures, Part-1: General Provisions and Buildings (Sixth Revision)" *Bureau of Indian Standard*, New Delhi.
11. Iwasaki, T., Arakawa, T and Tokida, K.I. (1984). "Simplified Procedure for Assessing Liquefaction During Earthquakes" *Soil Dynamics and Earthquake Engineering*, Vol. 3, No. 1, pp. 49-58.
12. Kramer, S.L. (2003). "Geotechnical Earthquake Engineering" *Pearson*.
13. LSTC (2009). "LS DYNA Keyword User's Manual- Release 971 R4*", Livermore Software Technology Corporation, Livermore*, California.
14. Maheshwari, B.K., Kaynia, A.M. and Paul, D.K. (2008). "Liquefaction susceptibility of soils in Himalayan region" *14 WCEE*.
15. Malhotra, P.K. (1999). "Response of Buildings to Near-Field Pulse-Like Ground Motions", *Earthquake Eng. Struct. Dyn.*, Vol. 28, No. 11, pp. 1309–1326.
16. Mammo, Tilahun (2005). "Site Specific Ground Motion Simulation and Seismic Response Analysis at the Proposed Bridge Sites within the City of Addis Ababa, Ethiopia", *Engineering Geology*, Vol. 79, pp. 127-150.
17. National Disaster Management Authority NDMA (2010). "Development of Probabilistic Seismic Hazard Map of India" Govt. of India, New Delhi.
18. Paul, G.S. (2005). "Engineering Characteristics of Near Fault Ground Motion" *NZSEE*.
19. Rakesh, K., Rao, G.R.S. and Prasad, D.S.V. (2016). "Seismic soil Liquefaction Susceptibility Assessment of District Krishna, Andhra Pradesh" *International Journal of Applied Research*, Vol. 2, No. 2, pp. 477-482.
20. Roy, N., Shuily, A., Sahu, R.B. and Jakka, R. S. (2018). "Effect of Uncertainty in V_s-N Correlations on Seismic Site Response Analysis". *J. Earth Syst. Sci., INAE,* Vol. 127:103, pp. 1-21.
21. Schnabel, P.B., Lysmer, J. and Seed, H.B. (2012). "Computer Program SHAKE: A Computer Program for Earthquake Response Analysis of Horizontally Layered Sites", *University of California*, Berkeley, California.
22. Seed, H.B. and Idriss, I.M. (1970). "Soil Moduli and Damping Factors for Dynamic Response Analysis" *Rep. No. EERC 84-14, Earthquake Engineering Research Centre, Univ. of California*, Berkeley, California, 40P.
23. Seed, H.B. and Idriss, I.M. (1981). "Evaluation of Liquefaction Potential of Sand Deposit Based on observation of performance in previous Earthquake" *ASCE National Convention, St. Louis, Missouri, USA, Preprint*, pp. 81-544.
24. Sesov, V., Edipn, K. and Cvetanovska, J. (2012). "Evaluation of the Liquefaction Potential by In-situ Tests and Laboratory Experiments in Complex Geological Conditions" *15 WCEE*.
25. Sitharam, T.G. (2007), "Evaluation of Liquefaction Potential of Soils" *Workshop on Micro Zonation* pp. 151-162.
26. Tokimatsu, K. and Yoshimi, Y. (1983). "Empirical Correlation of Soil Liquefaction Based on SPT-N Value and Fines Content" *Soils and Foundation*, Vol. 23, No. 4, pp. 56-74.
27. Uniform Building Code (1997). *International Conference of Building materials*, California, USA.
28. Youd, T.L. and Idriss, I.M. (2001). "Liquefaction Resistance of soil: Summary Report from the1996 NCEER and 1998 NCEER/NSF Workshops on Evaluation of Liquefaction Resistance of Soil" *Geotech and Geoenvironmental Engineering*, pp. 817-833.
29. Zachariah, J.P. and Jakka, R.S. (2021), "Accounting for the Uncertainties in the Estimation of Average Shear Wave Velocity Using V_s-N Correlations", *Front. Struct. Civ. Eng.*, Vol. 15, No. 5, pp. 1199-1208
30. Web source: www.strongmotioncentre.org site for near field and far field earthquake data. Last accessed on 15 April 2019.